An-Najah National University

Faculty of Graduate Studies

SYNTHESIS AND CHARACTERIZATION OF SILVER NANOPARTICLES USING PALESTINIAN THYMUS CAPITATUS, WITH EVALUATION OF ITS POTENTIAL ANTI-OXIDANT, ANTIMICROBIAL, ANTICANCER, AND ANTI-INFLAMMATORY ACTIVITIES

By

Lara Yassir Asmar

Supervisor

Dr. Ahmad Eid

This Thesis is Submitted in Partial Fulfillment of the Requirements for the Degree of Master of Pharmaceutical Science, Faculty of Graduate Studies, An-Najah National University, Nablus - Palestine.

2025

SYNTHESIS AND CHARACTERIZATION OF SILVER NANOPARTICLES USING PALESTINIAN THYMUS CAPITATUS, WITH EVALUATION OF ITS POTENTIAL ANTI-OXIDANT, ANTIMICROBIAL, ANTICANCER, AND ANTI-INFLAMMATORY ACTIVITIES

By

Lara Yassir Asmar

This Thesis was Defended Successfully on 06/3/2025 and approved by

Dr. Ahmad Eid	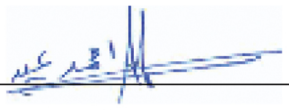
Supervisor	Signature
Dr. Hani Shtaya	
External Examiner	Signature
Dr. Mohammed Hawash	
Internal Examiner	Signature

Dedication

This thesis is dedicated to:

For the sake of Allah, my Creator, and the Lord whom we rely

My great teacher and messenger, Mohammed (May Allah bless and grant him), taught us the purpose of life

My homeland Palestine,

An-Najah National University, my second home

My academic advisers who guided me in this process

My father gave me the gift of dreams and the ability to realize them.

My mother taught me how to live this life and stand beside me until I became what I am now.

My husband who believed in my abilities

My Children: Abdullah, Kareem, and Rital, the light of my life, who gave me strength when I thought of giving up

My beloved brothers, especially Ibrahim, who gave me the courage to face life's challenges with confidence

All the people who encouraged and supported me to accomplish this work

Acknowledgements

First, I would like to express my heartfelt gratitude to Almighty Allah, who blessed me and reconciled me to accomplish this work and get the master's degree.

My sincere thanks go to my supervisor, Dr. Ahmad Eid, whose unwavering guidance and support were the cornerstone of my journey through this master’s program. His expertise and encouragement were pivotal in navigating this research and composing this thesis.

Also, I want to thank Dr. Nidal Jaradat and Dr. Mohyeddin Assali for their invaluable feedback and suggestions, which significantly enriched this work.

I am profoundly grateful to the support and resources provided by An-Najah National University, which created an optimal environment for research and scholarly exploration, and to all the participants in this study who share their time and experiences indispensably.

Finally, I sincerely appreciate my family's love, patience, and encouragement in completing my studies.

Declaration

I, the undersigned, declare that I submitted the thesis entitled:

SYNTHESIS AND CHARACTERIZATION OF SILVER NANOPARTICLES USING PALESTINIAN THYMUS CAPITATUS, WITH EVALUATION OF ITS POTENTIAL ANTIOXIDANT, ANTIMICROBIAL, ANTICANCER, AND ANTI-INFLAMMATORY ACTIVITIES

I declare that the work provided in this thesis, unless otherwise referenced, is the researcher's own work, and has not been submitted elsewhere for any other degree or qualification.

Student's Name: **Lara Yassir Asmar**

Signature: 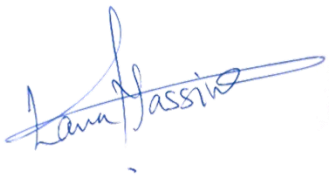

Date: **06/3/2025**

List of Contents

List of Tables

List of Figures

List of Appendices

SYNTHESIS AND CHARACTERIZATION OF SILVER NANOPARTICLES USING PALESTINIAN THYMUS CAPITATUS, WITH EVALUATION OF ITS POTENTIAL ANTI-OXIDANT, ANTIMICROBIAL, ANTICANCER, AND ANTI-INFLAMMATORY ACTIVITIES

By
Lara Yassir Asmar
Supervisor
Dr. Ahmad Eid

Abstract

Introduction: *T*his research that aimed to study the potential synthesis of silver nanoparticles utilizing *Thymus capitatus* essential oil as a reducing and stabilizing agent and to assess its potential biomedical applications.

Methodology: *T. capitatus* oil was hydrodistillated and characterized using GC/MS. The green synthesis of AgNPs included adding *T. capitatus* oil to 0.1 M AgNO3 aqueous solution. Synthesized AgNPs were characterized by UV-visible spectroscopy, dynamic light scattering, and atomic force microscopy. Both synthesized AgNPs and the oil were tested against six common bacteria. Different cell types were tested for cytotoxicity of the synthesized AgNPs and *T. capitatus* oil. The antioxidant activity was tested using DPPH. The COX inhibitor screening test investigated the anti-inflammatory effects of synthetic AgNPs and *T. capitatus* oil.

Results: In the (1.16 %) W/W oil extraction yield, carvacrol (37.47%), P-cymene (27.96%), and γ-terpinene (26.3%) were the primary chemical components After several trials to identify the optimal parameter, *T. capitatus* AgNPs were synthesized greenly. The final AgNPs colloidal sample was dark brown. UV-visible peak was 425 nm. The AFM image shows spherical AgNPs with a diameter of 40–80 nm. In contrast, DSL analysis showed an average effective diameter of 119.80 ±1.7 nm and a zeta potential of -43.86 ±2.2. *T. capitatus* oil and synthetic AgNPS outperform Trolox as antioxidants. Synthesized AgNPs outperformed *T. capitatus* oil by 5 times, with IC_{50} values of 2.27 ±0.91, 10.47 ±1.11, and 48.97 ±1.20 μg/ml for Trolox, AgNPs, and oil, respectively. Synthesized AgNPs outperformed *T. capitatus* oil by 5-folds against several bacterial

species, with MIC values ranging from 0.016 to 0.290 µg/ml for AgNPs and 0.078 to 1.562 µg/ml for pure oil. Both *T. capitatus* oil and produced AgNPs showed potential against HeLa, MCF-7, NIH3T3, Hep3B, and B16F1 cells. Synthetic AgNPs often (80%) at 200 µg/ml concentration. The oil and AgNPs were more selective for COX-2 than COX-1 and had considerable anti-inflammatory effects. The synthesized NPs showed a COX-2 IC_{50} value of 2.83 µg/ml, (14%) higher than the oil (19.42 µg/ml).

Conclusion: *T. capitatus* AgNPs has promising biomedical applications, particularly as potential agents in cancer therapy.

Keywords: Silver Nanoparticles; Carvacrol; *T. Capitatus*; Anti-cancer.

Chapter One
Introduction and Theoretical Background

1.1 General Project Overview

Herbal medications were first recorded by the Chinese people. They used different herbs to treat colds and miscellaneous diseases [1]. Nowadays, herbal medicine is known as modern herbalism (phytomedicine). Predominantly, traditional herbal medicine uses complex combinations of different medicinal plants [1].

Herbal extracts contain different pharmacologically active compounds, which are used for their antimicrobial, anti-inflammatory, antioxidant, antiviral, and antifungal activities [2] *Thymus capitatus (T. capitatus),* which grows in different regions in Palestine, is an herb used as an antibacterial, antiseptic, anthelmintic, antispasmodic, and carminative agent.

Recent clinical evidence suggests the use of herbal extractions in supportive therapy for cancer patients. For example, ginger roots can reduce chemotherapy-induced nausea, and *ginkgo biloba* minimizes lymphedema's symptoms after breast cancer therapy [3].

Recently, nanotechnology has been extensively researched in medicinal fields because of its unique chemical and physical properties. Bionanotechnology is an eco-friendly technology that solves major medical difficulties [4].

Silver salts have been found to have antiseptic activities and are used in many topical pharmaceutical formulations, such as creams for wound healing and burn treatment [5].

This work generated silver nanoparticles by green methods utilizing *Thymus capitatus* essential oil as the reducing agent. The biological activities of these AgNPs were comprehensively assessed, focusing on their antibacterial, antioxidant, anti-inflammatory, and anticancer properties.

1.2 Herbal medicine and essential oils

In recent decades, herbal medicine has become increasingly popular in many parts of the world. Herbal medicine needs to be taught to all healthcare practitioners. Numerous medicinal hypotheses have been proposed to explain this phenomenon, such as synergy,

enhanced bioavailability, and cumulative effects [1]. Herbal medicine has many advantages, including low cost, few side effects, high potency, and efficiency. On the other hand, there were some disadvantages, such as the inability to treat acute accidents, self-dosing risk, and the toxicity of some compounds [7].

A wide variety of plant components, including as buds, blossoms, leaves, seeds, stems, bark, and roots, can be used to extract volatile and aromatic chemicals known as essential oils. Extensive research on their possible use as an alternate therapy for a range of diseases is now in progress [1]. As an outcome of secondary metabolism in higher plants, they are produced by specialized secretory structures such glandular hairs and differentiated parenchyma cells [6]. EOs can be divided into two main chemical groups: terpenoids and, less commonly, phenylpropanoids [1]. These compounds exhibit many biological actions, including antioxidant and antibacterial properties. However, they have many undesirable physiochemical properties that reduce their use in medicine. For example, they are light-sensitive, highly volatile, have rapid degradation, and can produce undesirable flavors in the product. Moreover, their bioavailability is low [1, 8].

1.3 Description and literature review of *T. capitatus*

There are nearly 350 species of the genus Thymus that belong to the *Lamiaceae* family. Many types of thyme are used in herbal medicine worldwide [9]. However, they have been used as condiments and ornamentals. In herbal medicine, they are precious sources of essential oils that have been inspected for their antibacterial, anti-inflammatory, antioxidant, antiviral, antifungal, and sedative effects [2, 10]. Nowadays, the demand for thyme oil is growing because of the wide variety of its applications. *Thymus capitatus*, or *thymbra capitat*, is a species of wild thyme. It is a woody perennial plant native to the Mediterranean area, Turkey, and Europe.

It is commonly known as *conehead thyme* and *Spanish oregano* [11]. The plant has a length of 20–50 cm, with small, thin, dwarf shrub fleshy, green leaves that reach 12 mm in length, and pink flowers form conical clusters on the stem tips that reach 10 mm in length [12]. These flowers are protected by a layer of 6 mm-long reddish bracts fringed, and they typically bloom in summer. Moreover, *T. capitatus* is a hardy plant that can adapt to drought conditions. It flourishes in a dry, rocky environment, it can also be found in garrigue shrublands [8]. It grows in different regions in Palestine and is known by

different names according to the region, such as (Syrian thyme) in Tulkarem and (Zeatman) in Jenin and Nablus. Palestinians have used the aerial parts of the plant in salads or as a flavoring agent in cooked foods because of their pleasant and strong aromatic scent and pungent flavor.

Figure 1

Thymus capitatus plant

Traditionally, Thymus capitatus has been used in folk remedies due to its medicinal properties. It is used for several diseases and conditions , including digestive issues such as relieving bloating and to aid digestive, and respiratory problems such as coughs, colds, and bronchitis, because it is well known for expectorant activity [12]. Moreover, the EO is used in topical applications when diluted with a carrier substance to treat wounds and skin infections. It also relieves muscle pain and improves circulation [13].

Many studies reported that EO, which is extracted from *T. capitatus* leaves and its flowering tops, has strong antioxidant, anti-cancer, anti-inflammatory, and anti-microbial activities [13, 14].

T. capitatus essential oil exhibited antibacterial activity against a wide variety of bacteria, including both gram-negative and gram-positive strains. These bacteria included gram-negative *Klebsiella pneumoniae* and *Escherichia coli* and gram-positive *Listeria monocytogenes* and *Salmonella analum* It also has antifungal activity [15]. *T. capitatus* essential oil composition mainly consists of the phenolic monoterpene carvacrol, which

has strong anti-septic properties; other monoterpenes include p-cymene and γ-terpinene. Thymol, Linalool, 1,8-cineole, and others are present in fewer amounts [13].

Carvacrol is a monoterpenoid phenol found in the essential oils of numerous fragrant plants, including different species of thyme, and it has a pleasant smell and taste. It's recognized for its multiple pharmacological effects, including antibacterial, antioxidant, anti-inflammatory, and anticancer activity, due to its molecular structure (C10H14O), which features a hydroxyl group attached to a benzene ring.

Numerous studies have demonstrated that carvacrol exhibits antibacterial properties by disrupting bacterial cell membranes, leading to increased permeability and leakage of essential cellular components. Furthermore, its antioxidant action helps neutralize reactive oxygen species (ROS), hence lowering oxidative stress. Additionally, research reveals that carvacrol has anticancer characteristics, as it can trigger apoptosis in many cancer cell lines by influencing important biological pathways. For instance, Li et al. (2021) discovered that carvacrol effectively inhibits breast cancer-specific cells (BT-483, BT-474, MCF-7, MDA-MB-231, and MDA-MB-453) by DNA fragmentation, which downregulates the transient receptor potential cation channel as one of the anticancer mechanisms.

1.4 Nanotechnology in Medicine

1.4.1 Nanotechnology definition and history

The National Nanotechnology Initiative (NNI) describes nanotechnology as "the understanding and manipulation of matter at the nanoscale, within dimensions ranging from 1 to 100 nanometers, where unique phenomena give rise to innovative applications" [16]. This discipline may be employed across several areas, including biology, physics, chemical engineering, and medicine. In 1959, Nobel Laureate physicist Richard Feynman stated, "There is Plenty of Room at the Bottom" and suggested that materials and gadgets of the nanoscale scale might emerge in the future [17]. The term "nanotechnology" was originally introduced by Japanese scientist Norio Taniguchi in 1974, after being undiscussed prior to that year [18]. Nanotechnology emerged as a scientific area in 1982 with the introduction of the scanning tunneling microscope (STM) by Binnig and Heinrich Rohrer [19].

1.4.2 Applications of nanotechnology in medicine

Nanomedicine refers to the utilization of nanotechnology in medicine. It is based on several molecular technologies, including nanoscale-structured materials, devices, drugs, and other therapeutic agents, such as liposomes, micelles, polymeric nanoparticles, and dendrimers, that target different body sites [4, 20]. Some of the applications of nanomedicine include the antimicrobial activity of silver nanoparticles in health, dentistry, and the food industry, cancer therapy, immunotherapy, gene therapy, photothermal therapy, diagnostic devices, tissue repair, medical nanorobots, drug delivery, and biosensors [20].

The use of nanoparticles in cancer therapy allows for the targeted delivery of medications to individual cancer cells, which improves therapeutic efficacy while decreasing drug resistance and adverse effects. Moreover, nanomedicine enhances the solubility of some drugs with low water solubility, as a result, the efficiency of these drugs increases [21]. Nanomedicine is also used to synthesize scaffolds that enhance tissue regeneration. These scaffolds imitate the extracellular matrix in the body and support the growth and differentiation of stem cells [22]. Nanoscale devices can detect a specific biological condition or molecule at the nanoscale, helping diagnose and monitor a disease. Magnetic nanoparticles and quantum dots can enhance the contrast in different diagnostic imaging techniques such as CT scans, and MRI [4].

Another use of nanomedicine represents the improvement of existing vaccines or the creation of new ones. In 2016, the nanomedicine approach developed the first vaccine, when the contents of the conventional vaccine against toxoplasmosis, were encapsulated by nanoparticles [23]. Despite the multiple applications of nanomedicine, there are some risks combined with them, including development costs, toxicity to some normal cells, regulatory approval challenges, and limited information on the pharmacodynamics and pharmacokinetics of nanoparticles [24].

1.4.3 Classifications of nanomaterials used in nanomedicine

Nanomaterials that are used in nanomedicine are classified into three main groups.

A. Organic-based nanoparticles are based in their structure on organic liposomes, micelles, dendrimers, polymers, and proteins.
B. Inorganic-based nanoparticles, which can be divided into metallic nanoparticles such as silver and gold nanoparticles (AgNPs, AuNPs), respectively, metal oxide nanoparticles, for example; iron oxide, silicon oxide, and magnesium oxide nanoparticles. (Fe_2O_3NPs, SiO_2NPs, MgONPs), respectively, and quantum dots.
C. Carbon-based nanoparticles include nanotubes, fullerenes, and carbon-based quantum dots [25].

Recently, nanotechnology has been extensively researched in medicinal fields because of its unique chemical and physical properties. Bionanotechnology is an eco-friendly technology that solves major medical difficulties.

1.5 Silver Nanoparticles

1.5.1 Silver Nanoparticles Between the Past and Present

Silver is well-known for having antimicrobial activities. It was used to prevent the growth of many germs [26]. During World War I, wounds were wrapped in silver foil [27]. Recently, silver has been found in bandages and ointments as an antibacterial agent, allowing the wound to heal faster [28]. Furthermore, it is being applied to artificial bones and scaffolding to keep bones in place while mending [22].

Silver nanoparticles are recognized as the essential components of metal nanotechnology [29]. Silver nanoparticles are attracting significant attention in research because of their extensive range of applications in chemistry, microbiology, cell biology, pharmacology, and the food industry. Their distinct characteristics allow for application in various therapeutic approaches.

The synthesis of AgNPs may be classified into many methodologies, including top-down versus bottom-up, green versus non-green, and conventional versus nonconventional synthesis techniques [30].

Figure 2

Approaches of Silver nanoparticles synthesis [31]

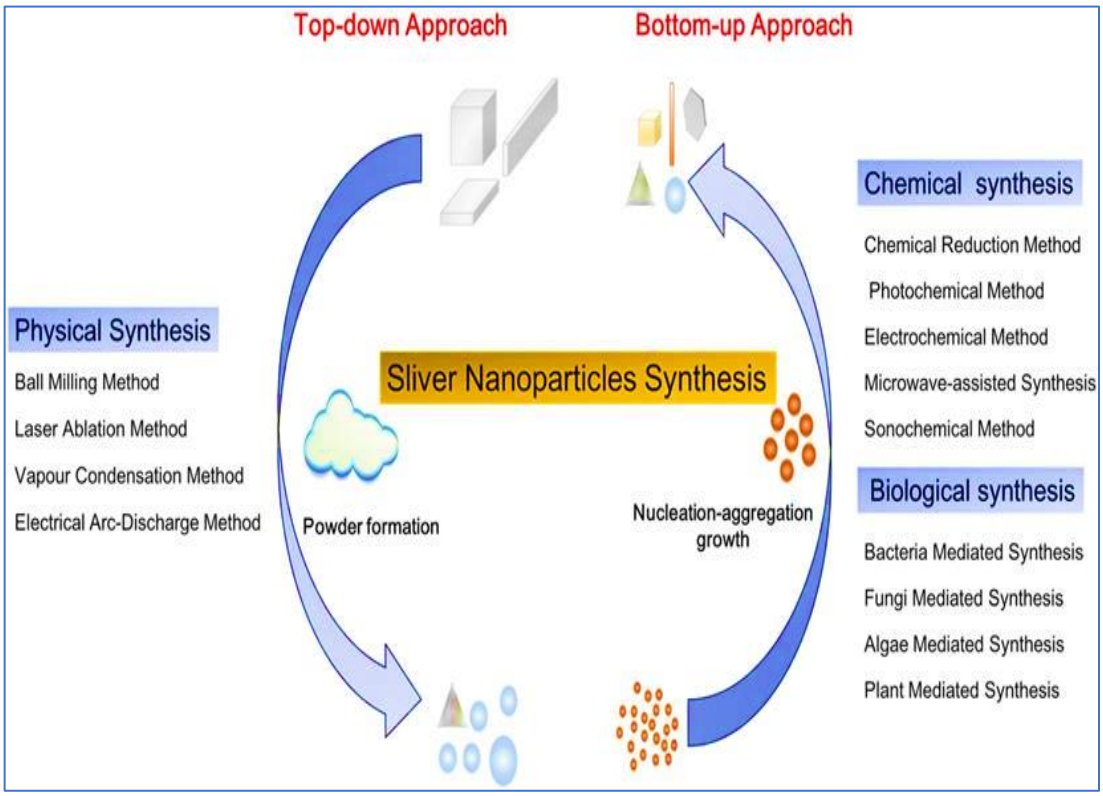

1.5.2 Green synthesis of silver nanoparticles: principles and examples

Green synthesis is the practice of using biologically and eco-friendly agents, including bacteria and plant fungi, to synthesize silver nanoparticles like plant extracts, bacteria, fungi, and other compounds for nanoparticle synthesis by applying a bottom-up approach [31]. The increasing acceptance can be attributed to two primary factors: its cost-effectiveness and energy-efficient characteristics, as well as the enhanced biological activity efficiency of nanosized particles from the plant extract compared to that of standard-sized extracts [32].

Green synthesis techniques for AgNPs typically involve two primary components: metal precursors and agents that decrease silver ions while stabilizing the colloidal nanoparticle system. Silver nitrate ($AgNO_3$) serves as the primary precursor for green synthesis. Additional silver salts, including silver perchlorate ($AgClO_4$) and silver tetrafluoroborate ($AgBF_4$), are employed in the chemical production of AgNPs [33].

The synthesis by plant extracts can be accomplished by using many plant parts, including seeds, leaves, and flowers. In literature, EO constituents such as flavonoids, terpenoids,

ketones, carboxylic acids, and amides can be used in the synthesis of silver nanoparticles due to their ability to reduce Ag^{+} to Ag^{0}. Furthermore, these constituents provide great antimicrobial properties to AgNPs [33, 34]. Green synthesis of AgNPs can be accomplished conventionally or by utilizing different external energy sources such as ultrasonic, electromagnetic, ultraviolet, visible, γ-radiation, and microwave radiation sources. Figure 3 shows the principle of the green synthesis of AgNPs [34].

Figure 3

The principle of green synthesis of AgNPs using plant extract

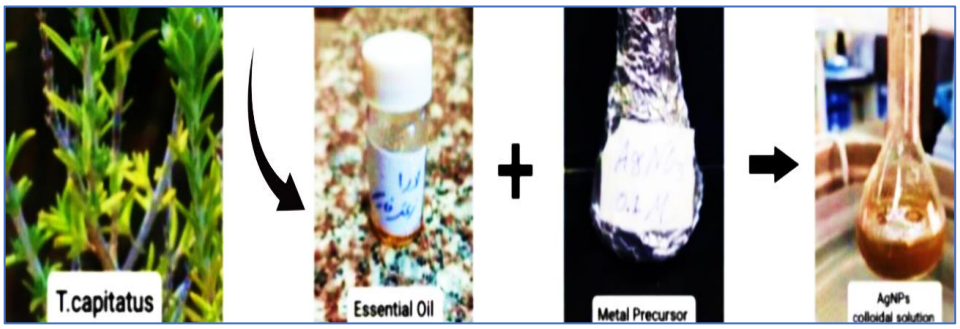

Numerous studies in the literature have highlighted the potential for green synthesis of silver nanoparticles using various plant extracts. For instance, pepper-leaf extract has proven to be an effective agent in this process, serving both as a reducing and capping agent for the synthesized AgNPs [35]. *Eugenia jambolana* leaf extract was a good choice for green synthesis because of the presence of flavonoids, alkaloids, and saponin compounds [36]. *Rhynchotechum elliptical* leaf extract was also used, as silver ions were reduced by alkaloids, flavonoids, terpenoids, and polyphenols [37]. In addition, many other reductants were used for AgNP synthesis. These were tarmac, cinnamon, red apple, egg white, mint, thymus vulgaris, sage leaves, lemongrass, coffee, and black tea [38].

1.5.3 Parameters that influence the green synthesis of silver nanoparticles

Several factors influence the AgNPs synthesis process, including temperature, pH, reaction duration, stirring time, silver precursor concentration, and concentration of plant extract [38]. The concentration of $AgNO_3$ aqueous solution is crucial in the synthesis of nanoparticles. An increase in $AgNO_3$ concentration results in a greater size and quantity of synthesized nanoparticles, while also reducing the reaction time. In essence, the reaction reaches an equilibrium state once all $AgNO_3$ particles have been consumed [39].

The concentration and constituents of the EO used are also major factors that affect the reaction time and the size and shape of synthesized NPs. It is believed that the oxidation reaction of different compounds of the plant extract is responsible for the reduction of Ag+ to Ag^0 [39, 40]. In addition, the hydroxyl group of varying chemical constituents is the major element for the reduction reaction [40]. Temperature is a crucial component influencing the production of nanoparticles, as it significantly determines their size and form. It is well recognized that elevated reaction temperatures enhance nucleation, leading to a rapid reduction of silver ions and the formation of many tiny spherical nanoparticles [39].

The synthesis of AgNPs is also influenced by the pH value of $AgNO_3$ aqueous solution. Several studies show that using an alkaline pH during AgNP synthesis leads to a steady, high production yield of NPs and reduces reduction time.

In other words, more OH groups can participate in the silver ion reduction process at a basic pH [41]. Several recent studies have successfully achieved the green synthesis of AgNPs using leaf extracts from *Curcuma longa*, *Solanum nigurum*, *Mentha aquatica*, *Cestrum nocturnum*, *Cleistanthus collinus*, and *Rhizoctonia solani*, which exhibited anticancer, antimicrobial, antiviral, and antifungal properties [42].

1.6 Biological activity of synthesized silver nanoparticles

The biological activities of AgNPs depend on their physiochemical properties such as particle shape, particle size, surface area, size distribution, morphology, and capping. These parameters affect the dissolution and agglomeration rates and the efficiency of ion release. Therefore, they influence the bioavailability of therapeutic agents by determining the biological distribution and cellular uptake and decreasing the effect of biological barriers [26, 34]. The particle size of silver nanoparticles affects the biological activity reversely, which means the smaller the particle size, the higher the activity due to the increasing surface area of the nanoparticles at the site of action. The spherical nanoparticles have the highest effect of biological activity due to the same reason.

To achieve the heights of biological activity of NPs, they must be uniform in size, morphology, and distribution. The nanoscale diameter enhances the interaction between nanoparticles and microorganisms, owing to their elevated surface area-to-volume ratio relative to bulk materials. As mentioned above, a smaller particle size correlates with

increased biological activity [26]. The mechanism of action of AgNPs, based on their antibacterial activity, involves their significant permeability through the bacterial cell wall. Furthermore, the release of Ag+ ions within the cytoplasm results in the disruption of cellular respiration, interference with ion exchange processes, and inhibition of bacterial protein synthesis on ribosomes. These effects illustrate the antibacterial efficacy of AgNPs and suggest their application as anti-pathogenic drugs [34].

The antimicrobial resistance property of many microorganisms is posing a serious life-threatening problem worldwide. However, the novel AgNPs with unique physiochemical properties possess potent antimicrobial activity, which plays an important role in antimicrobial and biomedical applications. The main principle underlying the antibacterial activity of synthesized AgNPs is not well established. Several recent studies have revealed that the released silver ions primarily cause the antimicrobial activity that damages cells. Furthermore, researchers have proposed several pathways for AgNPs' bactericidal activity, including the generation of free radicals, reactive oxygen species from AgNPs' surface, coating agents, damage to respiratory enzymes, and interactions with the bacteria's cell wall, all of which ultimately lead to a decrease in intracellular ATP levels [59, 60].

The anti-fungal activity of silver nanoparticles is similar to the mechanism of the anti-bacterial effect, it refers to the released Ag^{+} ions into the cytoplasm of the fungal cell disrupting the respiratory system and leading to cell damage [33]. The anti-viral mechanism of AgNPs is still unknown and needs further investigation. The antiviral activity of AgNPs is affected by variables like size, shape, and surface functionalization; however, in vitro tests have shown that these particles form a physical barrier against herpes simplex virus types 1 and 2, as well as human parainfluenza virus type 3 [43].

Approximately ten million patients passed away to cancer globally. By the year 2040, there will be approximately 27 million more cases of cancer globally [44]. Chemotherapy includes medications that originate from pharmaceutical compounds and plant extracts. These substances react with the metabolism of cancer cells, leading to death by preventing cell division. The anticancer activity of AgNPs has been widely studied. Many mechanisms of cytotoxicity can be included, mainly the generation of reactive oxygen species (ROS), which interact with the synthesis of microorganism proteins, furthermore, it was reported that the release of silver ions leads to mitochondrial damage in the cell, this action results in

autophagy and energy imbalance, so cell death occurs. The most important note is that the physical and chemical properties of AgNPs are the key elements of their biological activities that are implicated in their applications [32, 45, 46].

1.7 Hypothesis & significance for this project

This work is carried out to study the potential synthesis of silver nanoparticles (AgNPs) using Palestinian *Thymus capitatus* EO obtained by extracting dried leaves. We hypothesized that the chemically active components act as a stabilizing and reducing agent that reduces silver ions. The characterization of the formed AgNPs was done. Moreover, its potential antioxidant, anticancer, antibacterial, and anti-inflammatory activities were evaluated.

1.8 Objectives of the study

- To collect *T. capitatus* from different regions in Palestine.
- To extract *T. capitatus* essential oil by hydrodistillation technique using a Clevenger-type apparatus.
- To determine the chemical composition of the essential oil of *T. capitatus* extracted by GC/MS.
- To investigate the optimal method of green synthesis of silver nanoparticles (AgNPs) by applying different techniques.
- Characterization of produced silver nanoparticles (AgNPs) using ultraviolet-visible spectroscopy, dynamic light scattering (DLS), zeta potential, and atomic force microscopy (AFM)| analysis.
- To evaluate the antioxidant, antibacterial, anticancer, and anti-inflammatory activities of both *T. capitatus* EO and green synthesized AgNPs to provide a new biomedical agent that is a candidate in different treatment therapies, especially cancer therapy.

Chapter Two

Materials and Methods

2.1 General Methodology

This work used the hydro-distillation method to extract *T. capitates* EO. Many previous studies reported that it is better than other methods of extraction [47]. GC-MS was used to determine the chemical constituents of the EO. After that, several trials were applied to determine the appropriate technique to synthesize *T. capitatus's* AgNPs and the optimal parameters that affect the synthesis. The characterization of the obtained AgNPs was done using a UV-visible spectrometer, AFM, DLS, and a zeta potential analyzer. Finally, several *in vitro* biological tests were done on *T. capitatus* pure oil and synthesized AgNPs.

2.2 Materials and Chemical Reagents

The aerial parts of *T. capitatus* were gathered from multiple locations in northern cities in the West Bank, including Nablus, Tulkarm, and Jenin. The plant material was classified within the Pharmacy Department of An-Najah National University, designated with the code Pharm-PCT-A1729. The chemical reagents and materials used in this study were provided by the Faculty of Medicine and Health Sciences at An-Najah National University in Nablus. The liquids and solid chemical reagents employed in the experimental section are outlined in Table 1.

Table 1

Reagents and chemicals used for green synthesis of AgNPs, and laboratory assessments

Materials	Supplier	Country of supplier
Acetone, (DPPH) 2,2-Diphenyl-1picrylhydrazyl, methanol, Trolox ((s)-(-)-6 hydroxy-2,5,7,8-tetramethychroman-2-carboxylic acid), and Sodium Hydroxide Pellets,	Sigma-Aldrich	USA
Dimethyl sulfoxide (DMSO)	Riedel-de Haën	Germany
Silver Nitrate Powder	Nile Chemicals	India

Other reagents were provided by the laboratories of An-Najah National University in Nablus. These reagents include trypan blue solution, Hank's balanced solution, glutamine, trypsin, amphotericin B, analytical-grade RPMI 1640 culture medium, and lethal calf serum. penicillin, and streptomycin antibiotics. Cayman COX (human) Inhibitor Screening Assay Kit and Cayman ELISA Kit were used for anti-inflammatory evaluation. For cytotoxicity assessment, several cell lines were used, including:

- MCF-7 (Human breast cancer cell)
- NIH3T3 (Mouse embryonic fibroblast)
- HEK 293 (Human embryonic kidney cells)
- B16F1 (Mouse melanoma cells)
- HeLa (Cervical carcinoma cells)
- Hep3B (Human hepatocellular carcinoma)

For the antibacterial assay, six bacterial strains obtained from the American Type Culture Collection (ATCC) were utilized, including the following:

- MRSA
- Staphylococcus aureus (ATCC 6538)
- Klebsiella pneumoniae (ATCC 13883)
- Escherichia coli (ATCC 25922)
- Proteus vulgaris (ATCC 8427)
- Pseudomonas aeruginosa (ATCC 9027)

In addition, *Candida albicans* was employed to assess antifungal activity.

2.3 List of instruments used

An-Najah National University Laboratories in Nablus, Palestine, provided all of the instruments used in this study. Table 2 provides the necessary information.

Table 2

List of instruments used for green synthesis of AgNPs, and laboratory assessments

Instrument	Supplier	Country of supplier
Elmasonic S 100H	Elma Schmidbauer	Germany
PH Meter 3510	Jenway	UK
Balance - AS 220/C/2	Radwag	Poland
Shimadzu QP_5000GC-MS	Perkin Elmer	UK
UV. Spectrometer 3715	Jenway	UK
Atomic Force Microscopy (AFM) core	Nanosurf	Switzerland
NanoBrook Omni	Brookhaven	USA
Water bath -BPXOP1001040	Lab Teck	South Korea
Micropipettes	MRC, Ltd.	Israel
Microplate reader	UniLab	USA
96-Well plates	Greiner Bio one	North Americ
MHS-B Magnetic stirrer	ZENITHLAB	China

2.4 Collection of plant materials

On December 2023, aerial parts of *T. capitatus* were collected from different regions in Palestine. These aerial parts were dried in the shade for 15 days at the Pharmacy Laboratory of An-Najah National University, Nablus, Palestine.

2.5 Extraction process from *T. capitatus* leaves

The extraction of essential oils was conducted using hydrodistillation technique utilizing a Clevenger equipment. 250 grams of dried leaves were placed in a distillation flask, followed by the addition of distilled water to a total volume of one liter. The extraction procedure was conducted at atmospheric pressure at 100°C for a duration of 3 hours, with a hydro distillation rate of 0.54 ml/min. The EO was stored in the refrigerator at 4°C until used. The yield of EO from the facility was determined using the below calculation.

Yield percent = (Extract weight/Dry weight of *T. capitatus*) *100

2.6 Determination of the chemical composition of *T. capitatus* EO by Gas Chromatography/Mass spectrometry

The essential oil's chemical composition was analyzed using the GC-MS technique. GC-MS chromatograms were acquired using a Shimadzu QP-5000 GC-MS system, which featured a Rtx-5ms column with a length of 30 m, a film thickness of 0.25 µm, and an inner diameter of 0.25 mm. Helium functioned as the carrier gas, maintaining a flow rate of 1 mL/min. The injector temperature was held constant at 220°C. The oven temperature protocol commenced at 50°C for 1 minute, subsequently increased to 130°C at a rate of 5°C/min, followed by an elevation to 250°C at 10°C/min, and maintained isothermally for 15 minutes. The transfer line temperature was established at 290°C. Detection utilized an electron ionization system with a detector voltage set at 1.7 kV. The mass spectrometer functioned within a mass range of 38–450 m/z, featuring a scan rate of 0.5 seconds and a scan speed of 1000 amu/sec. The chemical components of the essential oil were identified via quantitative analysis of integrated peaks, utilizing comparisons of mass spectrometry retention times and Kovats indices with the NIST mass spectrometry database and pertinent literature references [48, 49].

2.7 Green synthesis of silver nanoparticles using *T. capitatus* extract

The synthesis of AgNPs was typically achieved through a bottom-up approach, utilizing an aqueous solution of silver nitrate ($AgNO_3$) as the precursor for silver ions. The diluted *T. capitatus* essential oil serves as a reducing agent for silver ions. Various approaches with distinct parameters were utilized to identify the most effective ones.

2.7.1 Precursor preparation

A solution of 0.1 M $AgNO_3$ was prepared using ultra-distilled water and was covered by aluminum foil because it is a photosensitive solution, then its' pH was adjusted to 8 using NaOH 0.1 mol/L solution, and it was kept in a dark place at room temperature until use [5].

2.7.2 Green Synthesis of AgNPs using *T. capitatus* EO

After precursor preparation, Acetone was used to dissolve *T. capitatus* EO (1:170 v/v) to achieve complete incorporation into the reaction system. After that, a dropwise addition of 2 mL of diluted oil to 20 mL of $AgNO_3$ solution was carried out with medium magnetic stirring for 20 minutes. Through the first 10 minutes of stirring, a reddish-brown color was observed, which indicates the reduction of silver ions (Ag^+ to Ag^0). At the end of the reaction (about 20 minutes), the color converted into dark brown, indicating the complete formation of nanoparticles. The process was accomplished at room temperature. The colloidal sample of AgNPs was stored at 4 ºC until use. In our procedure of synthesis, there was no need for a chemical stabilizer because compounds present in the EO act as stabilizing agents [50].

2.8 Characterization of AgNPs

Several techniques were applied to assess the characteristics of synthesized AgNPs from *T. capitatus* leaf extract. The reduction of Ag^+ ions was first confirmed by observing the reddish-brown color, followed by taking the absorbance from 200–800 nm in a UV–Vis spectrophotometer. Further characterization of the morphological properties of AgNPs was carried out through atomic force microscopy (AFM). Surface properties, dispersion state, and zeta potential were determined using the NanoBrook Omni particle analyzer.

2.8.1 Ultraviolet-Visible Spectroscopy Assay

The presence of silver nanoparticles in the suspended samples was approved by measuring the surface plasmon absorbance (SPA) using UV, a visible spectrophotometer with a quartz cuvette, employing wavelengths between 200 and 800 nm. For baseline correction, the 0.1 M $AgNO_3$ aqueous solution was used as a reference. This procedure was employed at room temperature [51].

2.8.2 Atomic Force Microscopy (AFM) Assay

A Core AFM (Nanosurf, Switzerland) was employed to examine the dispersion, aggregation, and morphological characteristics of the colloidal sample of synthesized AgNPs, including their shape. The samples were prepared by drop-casting a diluted solution of AgNPs onto mica substrates, followed by vacuum drying at 120°C [52]. The tapping mode utilized a probe force constant of 5 Nm^{-1} and operated at a resonance frequency of 150 kHz. The analysis of the photos was conducted using Gwyddion software [53].

2.8.3 Dynamic Light Scattering (DLS) and Zeta Potential Assay

A master size analyzer (Brookhaven Instruments, Nano Brook Omni, New York) was employed to assess the hydrodynamic diameter and dispersion of the produced AgNPs in the laboratory, using the principles of dynamic light scattering (DLS).

The trials were conducted at around 25°C, which is the standard room temperature. The results are shown as the average value plus or minus the standard deviation, based on a minimum of three measurements. For Dynamic Light Scattering (DLS) measurement, the cuvette was pre-rinsed with filtered solvent at least 3 times. The AgNP sample was filtered via a 0.2 µm membrane and loaded into a cuvette. The sample was placed into a cuvette with the smallest amount required.

The liquid level should be at least 2 mm higher than the instrument's laser beam entrance height. The cuvette was holed in the sample holder. Three independent measurements were performed. For Zeta Potential Measurement the cuvette was rinsed with water, then by methanol, and finally water again. The electrodes both inside and outside the measuring window were checked visually. Then, about 750 µL of synthesized AgNPs were added to the cuvette by syringe. The cuvette was holed in the sample holder. Three independent measurements were performed.

2.9 Antioxidant activity (DPPH) assay

The antioxidant activity of *T. Capitatus* EO was evaluated with a DPPH (2,2-diphenyl-1-picrylhydrazyl) test. The DPPH test has been thoroughly cited and corroborated in academic literature. The efficacy of *T. capitatus* EO and manufactured silver nanoparticles in scavenging free radicals was evaluated and compared to a positive control, Trolox. To prepare a Trolox (6-Hydroxy-2,5,7,8-tetramethylchroman-2-carboxylic acid) reference standard solution, dissolve 10 mg in 100 mL of methanol to get a concentration of 100 μg/mL. Additionally, two stock solutions of synthesized AgNPs and *T. capitatus* EO were produced independently in methanol at an identical concentration of Trolox.

Working solutions were prepared from each of the Trolox and stock solutions by serial dilution with methanol, yielding (2, 5, 10, 20, 50, 80, and 100 μg/mL). DPPH (0.002% w/v) solution was prepared by dissolving 2 mg of DPPH powder in 100 mL. DPPH must be prepared freshly because of photosensitivity. After that, the DPPH solution was combined with each working concentration and methanol in ratios of 1:1:1 to achieve a three-milliliter final volume. A blank solution was prepared by adding DPPH solution to methanol in a ratio of 1:2. All samples were incubated at room temperature for 30 min. in a dark place. A spectrophotometer was used to determine the absorbance value for each sample at a wavelength of 517 nm. The procedure was repeated three times [54, 55]. The antioxidant potential inhibition percentage of each sample was determined using this equation.

$$\text{DPPH inhibition \%} = (AB - Ats)/AB \times 100\% \quad (1)$$

Where AB: is the absorbance for the blank solution and Ats: is the absorbance of the tested sample.

2.10 Antimicrobial activity of synthesized AgNPs

2.10.1 Microorganisms utilized for antimicrobial assay

Six strains sourced from the American Type Culture Collection (ATCC) were employed in the antibacterial assay. These strains include *Klebsiella pneumoniae* (ATCC 13883), MRSA, *Staphylococcus aureus* (ATCC 6538), *Proteus vulgaris* (ATCC 8427), *Escherichia coli* (ATCC 25922), and *Pseudomonas aeruginosa* (ATCC 9027). Furthermore, *Candida albicans* was utilized for the assessment of antifungal activity.

2.10.2 Antimicrobial assay

The antibacterial efficacy of both manufactured AgNPs and *T. capitatus* EO was evaluated using the broth micro-dilution technique as per established protocols. The produced AgNPs and *T. capitatus* EO were dissolved in DMSO at a concentration of 200 µg/ml. Subsequently, 10 2-fold microdilutions of each solution were prepared in sterile Mueller-Hinton broth. The dilution was performed in an aseptic environment using 96-well plates. Subsequently, Micro-wells 1–11 were administered injections of the test microorganisms.

Micro-well number 11, containing sample-free Mueller-Hinton broth as a positive control for microbial growth, was utilized to assess antibacterial activity. Nonetheless, as a negative control, the Mueller-Hinton broth in micro-well 12 was devoid of any content. RPMI medium replaced Mueller-Hinton broth for the *C. albicans* test. Plates with bacterial strains were subsequently incubated at 35°C for a duration of 18 to 24 hours. In comparison, plates inoculated with *C. albicans* were incubated for 48 hours at a temperature of 35°C [57]. The minimum inhibitory concentration (MIC) was established by identifying the lowest concentration in the micro-well that exhibited no visible bacterial growth.

2.11 Cytotoxicity Assay

2.11.1 Types of Cell Lines cell used

In this study, several types of cell lines were used to assess the cytotoxic activity of synthesized AgNPs and *T. capitatus* EO, including MCF-7 (Human breast cancer cell), 3T3 (Mouse embryonic fibroblast), HeLa (Henrietta's cervical cancer), B16F1 (Mouse melanoma cells), HEK 293 (Human embryonic kidney cells), and Hep-3B (Human hepatocellular carcinoma).

2.11.2 Cytotoxicity assay

A cytotoxicity assay was conducted for both *T. capitatus* EO and the synthesized silver nanoparticles (AgNPs) based on a previously reported method with modifications. RPMI 1640 medium was supplemented with (1%) 2 mM l-glutamine, 50 IU/mL penicillin-streptomycin antibiotics, and 10% heat-inactivated fetal bovine serum (FBS). Carcinoma cells, following mycoplasma and bacterial removal, were cultured in RPMI 1640 medium with (10%) calf serum in a monolayer at 35°C.

Cells underwent three washes with phosphate-buffered saline (PBS). Following the removal of PBS, detachment was achieved using (0.025%) Trypsin-EDTA. RPMI 1640 medium was incorporated to reach a total volume of 10 mL. The cell suspension underwent centrifugation at 1000 ×g for a duration of 10 minutes, after which the resultant pellet was resuspended in 10 mL of medium. Cell viability was assessed utilizing the trypan blue exclusion method in conjunction with a hemocytometer, yielding a result that exceeded (96%). Stock cultures underwent weekly sub-culturing following inoculation. The cell line was cultured in 6-well tissue culture plates (9.8 cm^2) and maintained in a humidified atmosphere with (5%) CO_2 at 35°C. AgNPs and EO were applied to the cells independently. Following a 24-hour period, serial dilutions of the test samples were prepared at concentrations of 62.5, 100, 200, 400, 600, 800, and 1000 µg/mL, starting from an initial 0.1 mL sample. Absorbance for each well was quantified using a plate reader to evaluate cytotoxicity [55, 58]. The IC_{50} for each sample was compared to the IC_{50} for Doxorubicin positive control from the literature.

2.12 Anti-inflammatory Assay

The evaluation of the anti-inflammatory properties of the synthesized AgNPs and *T. capitatus* EO was conducted utilizing the COX (human) inhibitor screening assay kit provided by Cayman Chemicals (Item No. 560131). The procedure adhered to the manufacturer's guidelines, incorporating adjustments informed by prior research. Each inhibitor sample, comprising *T. capitatus* EO, the synthesized AgNP colloidal sample, and the positive control Ketoprofen, was dissolved in a minimal volume of dimethyl sulfoxide (DMSO) to achieve a final volume of 10 µL. Each prepared sample underwent incubation with a mixture of COX-1 or COX-2 enzymes in a diluted reaction buffer for a duration of 10 minutes at a temperature of 37°C. The reaction commenced with the addition of 10 µL of arachidonic acid, subsequently incubating at 37°C for exactly 2 minutes. The reaction was concluded by introducing 30 µL of stannous chloride solution into each tube, followed by a 5-minute incubation at room temperature. The amount of PGF2α generated in the COX reactions was measured through an enzyme-linked immunosorbent assay (ELISA).

The procedure entailed sealing a 96-well plate with plastic film and positioning it on an orbital shaker for incubation at room temperature for a duration of 18 hours. Following the incubation period, the plate underwent five washes with a prepared buffer solution. Two hundred microliters of Ellman's reagent were introduced, followed by an incubation period of 60 to 90 minutes at room temperature, ensuring that the well absorbance fell within the range of 0.3 to 0.8 at 405 nm. The absorbance was quantified utilizing a Unilab Microplate Reader 6000 alongside an ELISA plate reader. The inhibition percentage was determined by analyzing the results across different concentrations in relation to the ketoprofen control. The concentration-inhibition response curve facilitated the calculation of the IC_{50}, and the selectivity index (SI) was derived by dividing the IC_{50} of COX-1 by that of COX-2 [58].

2.13 Statistical analysis

Experiments were performed in triplicate, with results presented as mean values ± standard deviation (SD). Statistical significance was established with a *p*-value threshold of less than 0.05. P-values were computed using the t-test program, suggesting that the observed differences or effects were improbable to have arisen by chance, thus increasing the reliability of the findings. The IC_{50} value, indicating the concentration necessary for 50% inhibition, was assessed using BioDataFit version 1.02

Chapter Three

Results

3.1 Extraction yield of the collected EOs from T. capitatus

In this work, leaves of *T. capitatus* that were collected from different regions of Palestine (Nablus, Tulkarem, and Jenin) were subjected to the hydrodistillation method for extraction of the EO. According to previous studies, this method was more efficient than others for extraction. The percentage of extraction yield is shown in Table 3.

Table 3

The percentage yield EOs from T. capitates

Mass of sample (g)	% (w/w) EO
250	1.16

3.2 Determination of the chemical constituents of *T. capitatus* Essential Oil

Identification of the chemical constituents of *T. capitatus* EO was accomplished by GC-MS; it also determined their concentrations and elution orders, which reveal information about the volatile nature of oil. GC-MS analysis of EO constituents showed about twenty compounds that were separated and identified, mainly monoterpenes such as carvacrol, p-cymene, thymol, and terpinenes, others such as sesquiterpenes (Caryophyllene). Major compounds were carvacrol (37.47%), which had the highest percentage, followed by p-Cymene, (27.96%), and ɣ-terpinene (26.3%). According to GC-MS analysis, major compounds of *T. capitatus* EO are shown in Table 4.

Table 4

Percentage of chemical constituents of T. capitatus EO determined by GC-MS analysis

Compounds	(Rt)	Composition (%)	KRI	LKRI
α-Thujene	8.42	0.09	925	923
Camphene	9.4	0.12	949	952
α-Pinene	9.76	0.16	930	932
α-Phellandrene	11.26	0.02	1006	1002
Sabine	11.73	0.05	969.7	970
β-Myrcene	12.33	0.65	987.8	987
Terpinolene (δ-terpinene)	13.49	1.73	1082	1083
p-Cymene	13.83	27.96	1021	1022
Limonene	14.03	0.29	1026.7	1026
Moslene (ɣ - terpinene)	15.29	26.3	1056.2	1056
Linalool	17.05	0.59	1097.4	1097
Cis- β- Terpinol	17.86	0.07	1141.7	1043
Terpinen-4-ol	20.2	0.11	1173.2	1172
Thymol	23.67	0.29	1293	1290
Carvacrol	24.3	37.47	1304	1300
β- Caryophyllene	26.98	0.21	1417.2	1418
Caryophyllene	28.55	2.28	1586	1580
Total Sum		98.39		

3.3 Green synthesis of silver nanoparticles using *T. capitatus* extract

The optimal synthesis of silver nanoparticles is influenced by several parameters, including the concentration of $AgNO_3$ aqueous solution, the concentration and chemical composition of *T. capitatus* EO, the pH of the $AgNO_3$ solution, and the temperature of the reaction. The concentration of $AgNO_3$ aqueous solution must keep the reaction in an equilibrium state. In our study, the optimal $AgNO_3$ concentration was 0.1 M. At this concentration, the reaction time was about 15 minutes. The initial analysis of AgNP formation revealed a reddish-brown hue within the first ten minutes of the reaction.

However, at the end of the reaction, the color became dark brown. Figure 5 illustrates the color changes.

To achieve optimal oil incorporation in the reaction system, the optimal EO concentration (1:170 v/v) was diluted in acetone. Temperature is a crucial parameter in the synthesis of nanoparticles as it influences the determination of particle size and shape. During our study, we observed that high temperatures led to spherical and large particles with diameters of 200 nm, which is not acceptable in our work. Conversely, low temperatures gave smaller particle diameters with triangle shapes, which was not acceptable either, because we aimed to get particles with diameters of less than 100nm and a spherical shape that has the highest biological activity. Moreover, we observed that a high concentration of silver ions increased the yield of nanoparticles with a spherical shape; in contrast, at lower silver ion concentrations, the yield was lower with different particle shapes. However, we resolved this issue by conducting the reaction at room temperature with a high $AgNO_3$ concentration of 0.1 M.

The pH of the AgNO3 solution plays a crucial role in the synthesis of NP. Numerous investigations have shown that employing an alkaline pH in the synthesis of AgNPs leadsto a stable and high yield of nanoparticles, while simultaneously decreasing the reduction time. In our study, the pH range of 5.4_6.5 was slightly acidic, making it difficult to form NPs. Therefore, we adjusted the pH to 8 using a 0.1 M NaOH aqueous solution. By determining previous parameters, we had a colloidal sample of AgNPs with a spherical shape and a diameter range between 40 and 80 nm.

Figure 4

Color changes during green synthesis AgNPs from T. capitatus EO

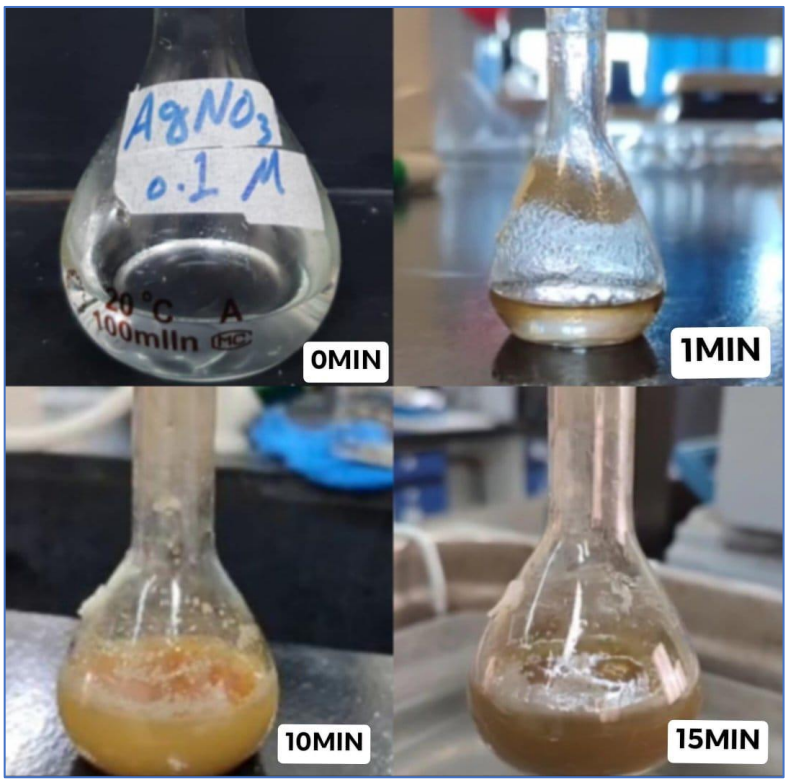

3.4 Characterization of synthesized *T. capitatus* AgNPs

3.4.1 Characterization by UV–Visible spectrophotometer

The secondary investigation of AgNPs synthesis utilized a UV-Vis spectrophotometer for analysis. Initially, we observed a pale-yellow color shift in the $AgNO_3$ aqueous solution when we added the diluted EO. The spectral absorbance of the synthesized AgNPs colloidal solution was monitored weekly at the wavelength of 200–800 nm. For each analysis, the peak was the same, obtained at 425 nm at which the absorbance was (1.020357711) as shown in Figure 5. Therefore, the synthesized AgNPs sample was stable for about 12 weeks at 4°C in a refrigerator. Figure 6 displays the spectral analysis peak of synthesized AgNPs.

Figure 5

UV–Visible absorption spectra of synthesized AgNPs

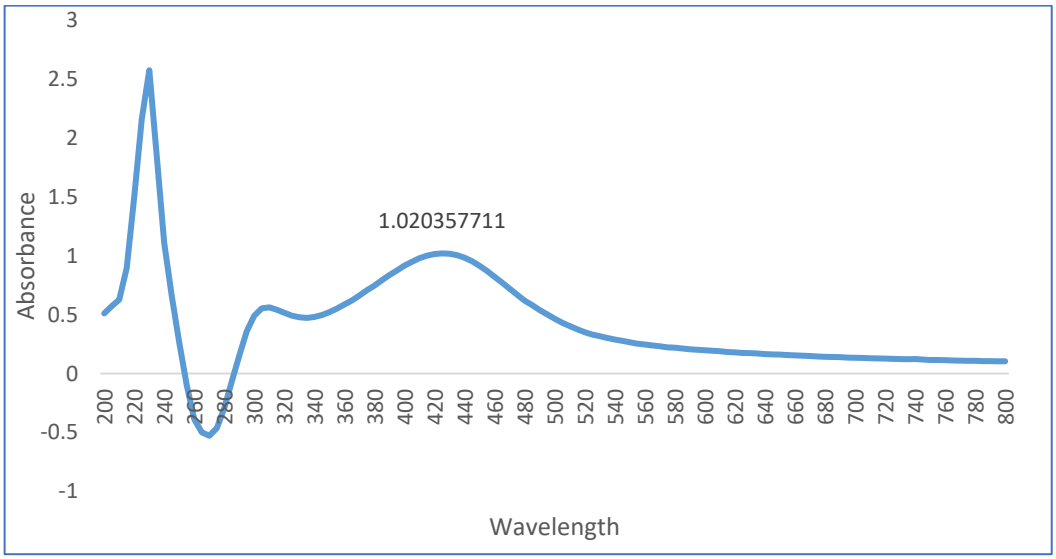

3.4.2 AFM image of *T. capitatus* EO synthesized AgNPs

The AFM image shows a mostly spherical shape of the synthesized AgNPs with a diameter of 40–80 nm, which was smaller than the result obtained by DLS measurements.

Figure 6

AFM image of synthesized T. capitatus AgNPs

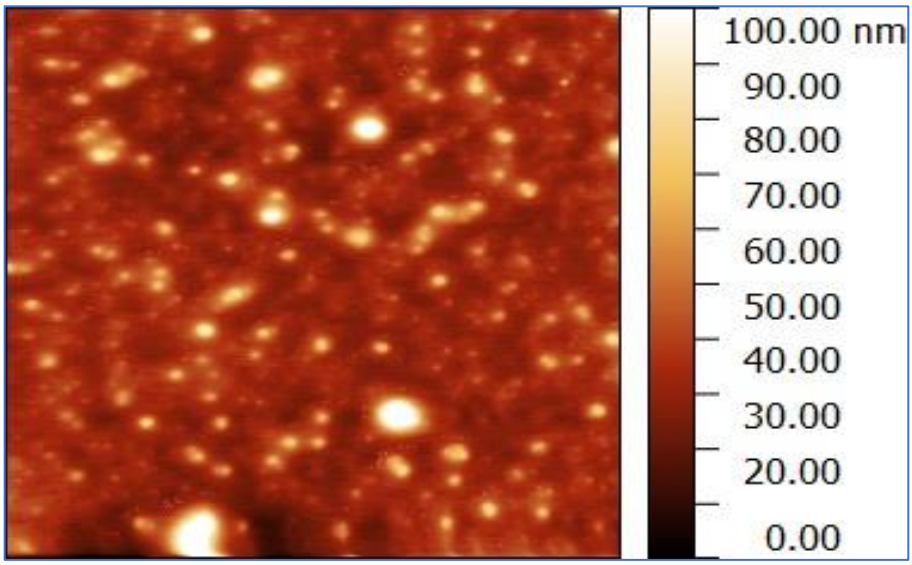

3.4.3 DLS and Zeta Potential of *T. capitatus* EO synthesized AgNPs

The DLS and zeta potential values of the synthesized AgNPs are shown in Table 5. The average effective diameter was 119.80 ±1.7 nm, and the average polydispersity was 0.220 ±0.04, showing the range of particles evenly spread out.

Table 5

DLS and zeta potential analysis of synthesized T. capitatus AgNPs

Particle size (nm)	Polydispersity Index	Zeta Potential (mV)
119.80 ±1.7	0.220 ±0.04	-43.86 ±2.2

3.5 Antioxidant Evaluation of *T. capitatus* EO and its Synthesized AgNPs

The DPPH assay was used to evaluate the antioxidant activity of both synthetic AgNPs and *T. capitatus* EO. DPPH is a stable radical that exhibits a purple hue when dissolved in methanol, with its absorption maximum recorded at 517 nm through UV-visible spectroscopy [55]. The antioxidant assessment approach is based on the color conversion of the DPPH solution from purple to yellow, which signifies that the maximal absorbance disappears when DPPH is reduced by an antioxidant. Figure 7 shows *T. capitatus* EO and synthesized AgNPs antioxidant activity, as well as their percent inhibition at various doses (0-100 µg/ml). Both *T. capitatus* EO and synthesized AgNPs have excellent antioxidant activity. However, the antioxidant activity of synthesized AgNPs is greater than the EO by about twofold. Table 6 displays the IC_{50} values for EO and AgNPs compared to the reference Trolox.

Table 6

The IC_{50} values of antioxidant activity for T. capitatus EO and its T. capitatus AgNPs compared to the reference Trolox

Sample	IC_{50} values (µg/ml)
Trolox	2.27 ±0.91
T. capitatus EO	48.97 ±1.20
Synthesized AgNPs	10.47 ±1.11

Figure 7

The antioxidant activity of T. capitatus EO and its synthesized T. capitatus AgNPs compared with trolox (positive control)

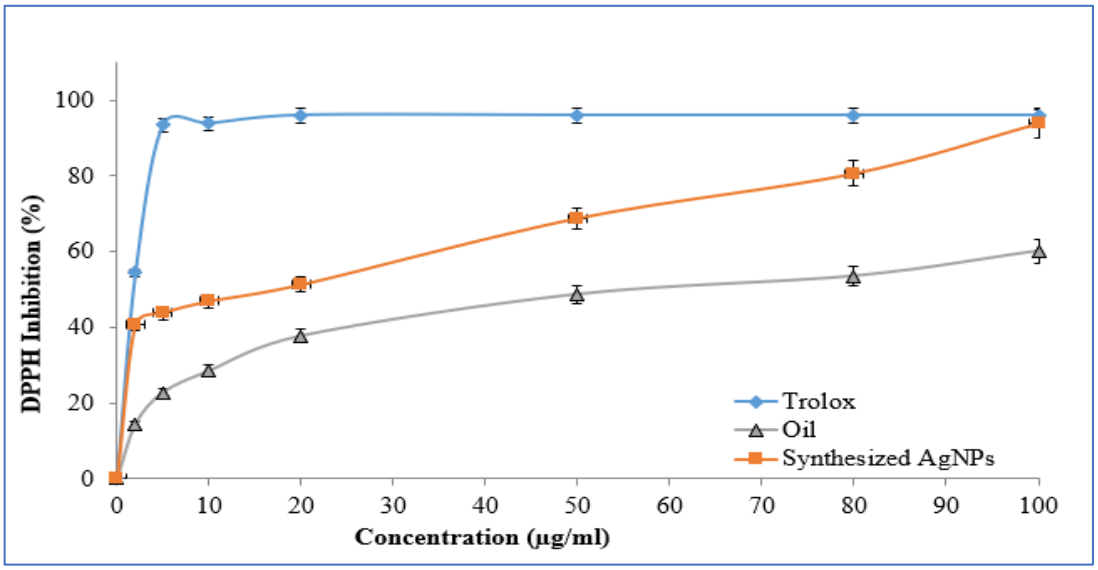

3.6 Antimicrobial evaluation of *T. capitatus* EO and its synthesized AgNPs

In vitro, antimicrobial assay for *T. capitatus* EO and synthesized AgNPs was performed by using the broth micro-dilution method according to a previous protocol in the literature, with some modifications [56]. The synthesized AgNPs outperform *T. capitatus* pure oil in their potency against both gram-negative and gram-positive bacteria, according to the results. Table 6 displays the Minimum Inhibitory Concentration (MIC) values. Despite the MRSA strain's resistance to most antibiotics, the EO and synthesized AgNPs were highly effective against it.

The minimum inhibitory concentration (MIC) is defined as the lowest concentration that prevents the observable growth of microorganisms *in vitro*. The MIC values for the synthesized AgNPs against the tested bacterial strains ranged from 0.130 ±0.001 µg/ml to 0.290 ±0.004 µg/ml, while for *C. albicans*, the value was 0.016 ±0.00 µg/ml. The MIC values of the oil are observed to range from (0.625 ± 0.002 µg/ml to 1.562 ± 0.004 µg/ml) when tested against six prevalent bacterial strains, and (0.078 ± 0.00 µg/ml) for *C. albicans*.

Table 7

MIC values for anti-microbial assay of T. capitatus EO and synthesized AgNPs

Microorganism	*T. capitatus* EO MIC	Synthesized AgNPs MIC
MRSA	1.562 ± 0.004	0.230 ± 0.001
S. aureus (ATCC 25923)	0.781 ± 0.002	0.131 ± 0.002
K. pneumonia (ATCC 13883)	1.562 ± 0.002	0.290 ± 0.004
E. coli (ATCC 25922)	0.781 ± 0.003	0.156 ± 0.00
Proteus. Vulgaris	0.781 ± 0.004	0.191 ± 0.00
P. aeruginosa (ATCC 9027)	0.625 ± 0.002	0.130 ± 0.001
Candida albicans (ATCC 90028)	0.078 ± 0.00	0.016 ± 0.00

3.7 Cytotoxicity evaluation of *T. capitatus* EO and its synthesized AgNPs

The anti-cancer activity of *T. capitatus* EO was assessed in several previous studies. Furthermore, many researchers confirmed that silver nanoparticles that are synthesized from plant extract have potent anti-cancer activity [15, 59, 60]. In this study, different cultural cell lines were used, including HeLa, MCF-7, NIH3T3, HEK 293, Hep_3B, and B16F1 cells. Each cell line was subjected to increasing quantities of the pure oil and synthesized AgNPs separately (1000, 800, 600, 400, 200 μg/ml) for 24 hrs. Finally, the MTS test was used to get a quantitative reading on the cell viability.

Results show both *T. capitatus* EO and synthesized AgNPs have great anticancer activity against the cell lines mentioned above. Also, it shows that as the concentration of pure oil and AgNPs increases, the percent inhibition increases too. Figure 9 shows the percentage inhibition for both *T. capitatus* essential oil and synthesized AgNPs. Synthesized AgNPs show more than 80% inhibition against hepatocellular carcinoma (Hep_3B) and melanoma cancer cells (B16F1) at concentrations less than 200 μg/ml. However, other inhibition percentages of synthesized AgNPs are around 80% at a concentration of 200 μg/ml or a little above it. According to IC_{50} values, which are shown in Figure 8, the potency of AgNP activity is higher than *T. capitatus* EO. IC_{50} values against HeLa cells were 38.9 μg/ml for T.capitatus oil, and 25.11 μg/ml for synthesized AgNPs, against MCF-7 they were 33.41 μg/ml for oil and 22.9 μg/ml for synthesized AgNPs, against 3T-3 they were 27.54 μg/ml for oil and 18.19 μg/ml for AgNPs, against HEK they were 21.87 μg/ml for oil and 18.19 μg/ml for AgNPs, against Hep-3B they were 31.62 μg/ml for oil and 22.38 μg/ml for synthesized AgNPs., finally against B16F1 they were 33.65 μg/ml

for oil and 27.54 µg/ml for AgNPs. These values were compared with the IC_{50} values of doxorubicin that were reported in previous studies in the literature.

Figure 8

The mean IC_{50} (SD ±0.5) of T. capitatus EO and synthesized AgNPs on different types of cancer cell lines

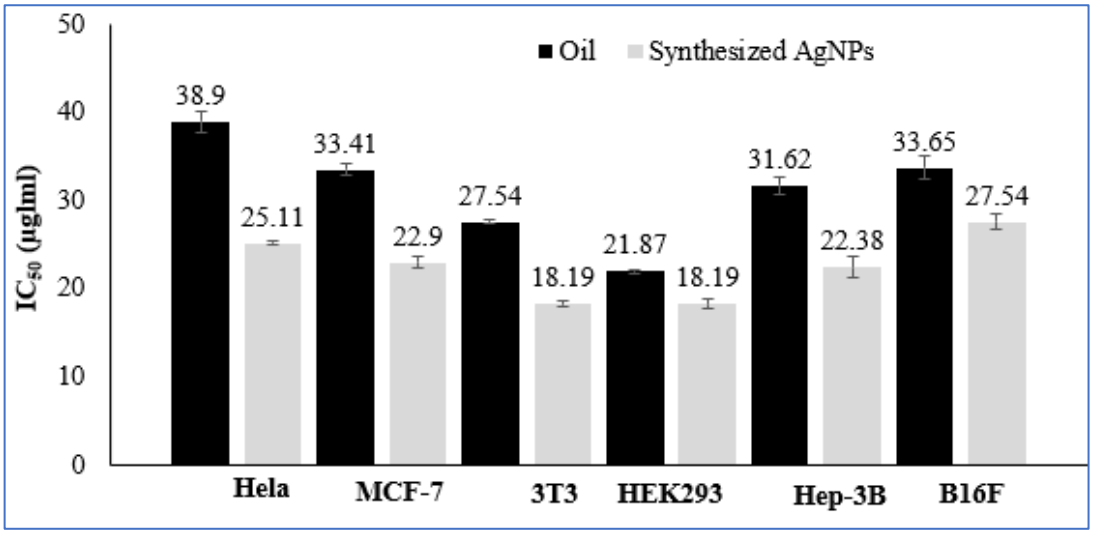

Figure 9

Percent inhibition of T. capitatus EO and synthesized AgNPs against different types of cancer cell lines

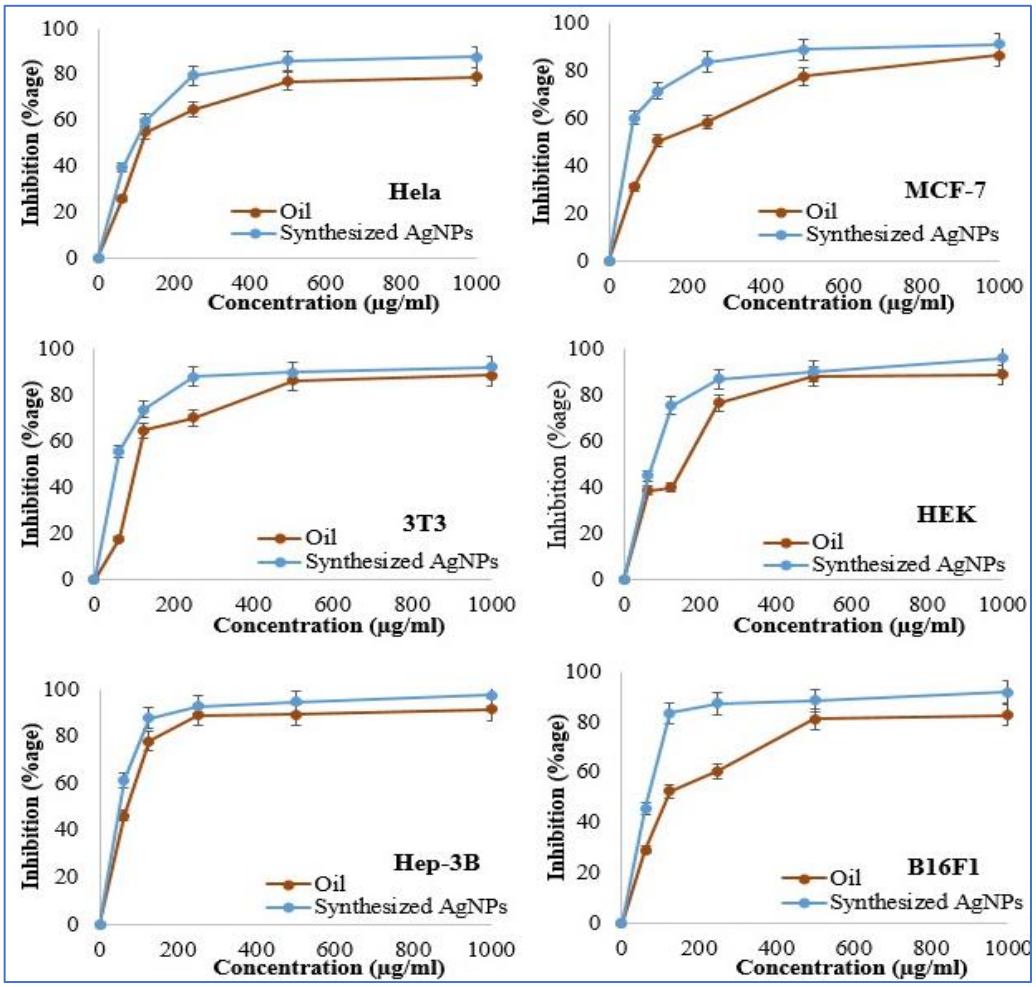

3.8 Anti-Inflammatory evaluation of *T. capitatus* EO and its synthesized AgNPs

Inflammation is a process by which the body responds to a stimulus that activates the immune system and enhances the production of anti-inflammatory mediators such as cytokines, chemokines, and COX-1 and COX-2 isozymes [61]. Many drugs are being used as anti-inflammatory agents. Because of their side effects, there is a need to find alternatives with higher effectiveness and fewer side effects, so several studies have been done on plant extract and its derivatives

We assessed the anti-inflammatory activity of *T. capitatus* EO and its synthesized AgNPs separately against the cyclooxygenase isoenzymes COX-1 and COX-2 in this work. It was found that synthesized AgNPs have strong anti-inflammatory properties. Their IC_{50} values are 7.71 ±0.5 µg/ml for COX-1 and 2.83 ±0.5 µg/ml for COX-2. This is higher

than the pure oil's values of 23.7 ±0.5 µg/ml for COX-1 and 19.42 ±0.5 µg/ml for COX-2. Whereas the positive control (ketoprofen) has IC_{50} values of 7.89 ±0.5 µg/ml and 40.18 ±0.5 µg/ml.

Table 8 displays the selectivity index values of synthesized AgNPs, *T. capitatus*, and the positive control (Ketoprofen). The synthesized AgNPs and pure oil were both better at targeting COX-2 than COX-1. The synthesized NPs were even better at targeting COX-2, with an IC_{50} value of 2.83 µg/ml, which was almost 14% higher than the oil's IC_{50} value of 19.42 µg/ml. In addition, the AgNPs's IC_{50} toward COX-2 (2.83 µg/ml) was almost 7% of the value for Ketoprofen (40.18 µg/ml).

Figure 10

In vitro COX1/COX2 inhibition (IC50 ±0.5 µg/ml) of T. capitatus EO and its synthesized AgNPs compared with Ketoprofen (positive control)

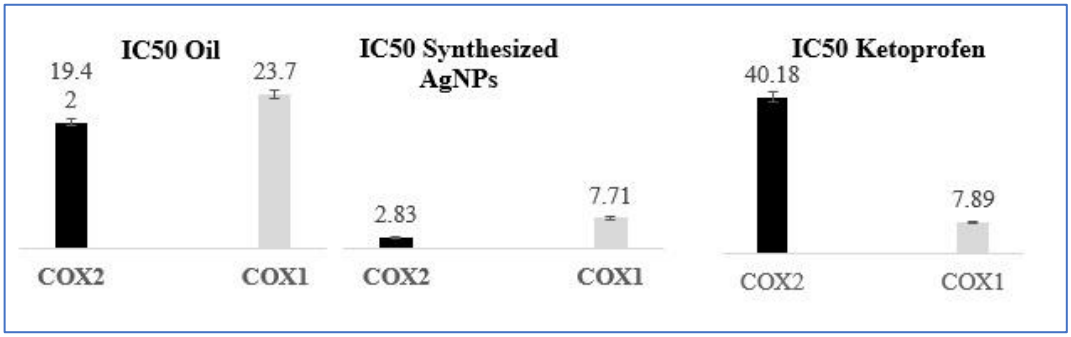

Table 8

The COX2 selectivity index for T. capitatus EO and its synthesized AgNPs compared with Ketoprofen (positive control)

Compounds	COX2 selectivity index
Oil	1.22
Synthesized silver nanoparticles	2.72
Ketoprofen	0.19

Chapter Four

Discussions

4.1 The extraction yield of the EO from *T. capitatus* leaves

The hydrodistillation technique was employed in our work to recover the desiccated aerial components of *T. capitatus* from different areas in Palestine. Research indicates that this approach surpassed alternative extraction methods [47]. As shown in the results, the yield was (1.16% w/w). this result emphasizes the previous result of Tunisia *T. capitatus* whose yield was (1.26%) [62]. On the other hand, *T. capitatus* from Morocco provides a yield of (2.6 ± 0.1%) [63]. Comparing the results of prior research to those acquired in this work, we can infer that the *T. capitatus* EO yield is high, indicating that it will contribute to being a key plant source on an industrial pharmaceutical scale. Several factors influence the EO yield, including the age of the plant, the harvest period and location, and the drying and extraction methods [9].

4.2 Constituents of *T. capitatus* Essential Oil

The GC-MS analysis of *T. capitatus* EO constituents revealed the separation and identification of about twenty compounds, primarily monoterpenes and sesquiterpenes in varying percentages. The major chemical constituents were carvacrol (37.47%), which had the highest percentage, followed by p-cymene (27.96%), and g-terpinene (26.3%). On the other hand, camphene (0.12%), a- pinene (0.16%), thymol (0.29%), caryophyllene (2.28%), and terpinilone (1.73%) appeared in lower concentrations. This result aligns with the findings of a previous study done on Tunisian *T. capitatus* by Amira Zaïri and others, which reveals about 25 compounds including Carvacrol (65.38%), P-cymene (6.25%), and g-terpinene (6.75%) [64]. However, another study was done in Algeria that showed *T. capitatus* contains 28 compounds [65]. There were several noticeable differences in the main chemical constituent percentage [11]. Several factors contribute to these variations, including the plant's origin, weather circumstances, soil components, harvest timing, and genetic variables [66]. The main chemical components of *T. capitatus* EO in Algeria, as reported in a prior research, are listed in Appendix B.1 [67].

4.3 Green synthesis of silver nanoparticles

The possibility of green production of silver nanoparticles utilizing various plant extracts from different areas of the plant has been the subject of several previous research efforts. A change in color was the primary endpoint of the initial studies examining AgNPs reduced to silver ions [50]. Initially, the colorless AgNO3 solution became colored upon the addition of diluted *T. capitatus* EO. Within the first 10 minutes of the reaction, the color changed to reddish-brown, and finally, within 15 minutes of the reaction under medium magnetic stirring at room temperature, it transformed to dark brown. This obtained result was aligned with the results of the green synthesis of AgNPs using the leaf extracts from *Solanum nigurum*, *Curcuma longa*, *Mentha aquatica*, *Cestrum nocturnum*, *Cleistanthus collinus*, and *Rhizoctonia solani* and displayed antimicrobial, antifungal, antiviral, and anticancer activities [42].

Several parameters determined the optimal synthesis of silver nanoparticles, including the concentration of $AgNO_3$ aqueous solution, the concentration and chemical constituent of *T. capitatus* EO, the pH of the $AgNO_3$ solution, the temperature of the reaction, and the stirring time.

In the process of making NP, the amount of $AgNO_3$ in the water is very important. It was discovered that as the $AgNO_3$ concentration rises, the size and number of synthesized NPs also rise, and the reaction time decreases [33]. This means that the reaction will be in an equilibrium state when all the $AgNO_3$ particles are used up. In our study, the optimal $AgNO_3$ concentration was 0.1 M. The observation of the color changing into dark brown confirmed the reaction time of about 15 minutes at this concentration. However, the first investigation to confirm AgNP nucleation was the reddish-brown color observed within the first ten minutes of synthesis. All previous studies of the green synthesis of AgNPs using plant extract showed a color change.

The concentration and constituents of the EO used are also major factors that affect the reaction time and the shape and size of synthesized NPs. The oxidation reaction of various compounds within the plant extract is thought to encourage the reduction of Ag^+ to Ag^0. In addition, the hydroxyl group of different chemical constituents is the major element for the reduction reaction [68]. In this research, the optimal EO concentration was (1:170 v/v) diluted in acetone to accomplish the complete incorporation of EO into the reaction

system. This diluted extract concentration was the same in a study that synthesized AgNPs using Oregano, thyme, clove, rosemary, and Poiretia latifolia leaves extract, which was done by Matheus Vinicius and others [69]. We emphasize that the hydroxyl group of the compound carvacrol (a phenolic monoterpene), which has the highest percentage (37.27%), is the main chemical group responsible for the reduction reaction of silver ions.

The synthesis of nanoparticles is significantly influenced by temperature, which plays a crucial role in determining their size and shape [50]. It is well established that increasing reaction temperatures will promote nucleation, resulting in a quick reduction of silver ions and forming small spherical NPs in large numbers[70]. As we were studying this parameter, high temperatures resulted in large particle diameters, but we solved this problem by accomplishing the reaction at room temperature with a high $AgNO_3$ concentration (0.1 M), resulting in spherical NPs with diameters between 40 and 80 nm, as determined by AFM analysis.

The pH value of the $AgNO_3$ aqueous solution also influences the synthesis of AgNPs. Several studies showed that using an alkaline pH during AgNP synthesis leads to a steady and high yield of NPs while reducing reduction time. A basic pH increases the number of OH groups engaged in the silver ion reduction process [71]. The pH of the $AgNO_3$ solution in our study was slightly acidic (pH 5.7), which made it difficult for NPs to form.

We worked at different pH levels by utilizing NaOH 0.1 mol/L. At pH of there were no particles formed, and this was confirmed by a UV-visible spectrometer graph. There weren't any peaks at the nanoparticle range. At 9 pH, the silver particles that formed were with a diameter of 200 nm and more, which is not acceptable. At 11 pH, a bulk of silver metal was formed instead of silver nanoparticles, and that was visually detected and confirmed by UV-visible spectrometer, which detected noises on the graph. The optimal pH was 8, which made the formation of spherical NPs with a diameter less than 100 nm. This aligns with the research conducted by Matheus Vinicius and colleagues, who modified the pH to 8 by utilizing NaOH 0.1 mol/L during the synthesis of AgNPs with extracts from oregano, thyme, clove, rosemary, and Poiretia latifolia leaves [69].

By determining the previously mentioned parameters, we had a colloidal sample of *T. capitatus* AgNPs with a dark-brown color, which was kept in the refrigerator at 4°C until use for in vitro biological activity. Furthermore, numerous recent studies have achieved the effective green synthesis of AgNPs utilizing leaf extracts from *Solanum nigurum*, *Curcuma longa*, *Mentha aquatica*, *Cestrum nocturnum*, *Cleistanthus collinus*, and *Rhizoctonia solani*, demonstrating anticancer, antimicrobial, antifungal, and antiviral properties. [42].

4.4 Characterization of AgNPs

4.4.1 Characterization by UV-Vis spectrophotometer

UV–Vis spectrophotometer was used for the secondary investigation of AgNP synthesis. The first investigation was the changing of the color that was observed during the reaction between *T. capitatus* extract and AgNO aqueous solution. The absorption spectra of synthesized AgNP colloidal samples were monitored by recording the peaks at a wavelength range of (200–800 nm). Several investigations revealed that AgNP's spectral peak varied from (410-430 nm). In our study, there was only a single SPR band, and the peak was achieved at 425 nm, indicating that the manufactured NP has a spherical form, and this crystal structure has been confirmed in the AFM image. Our findings are similar to those published in research on green AgNP production employing the microbial species Rhizopus stolonifera, which showed the highest absorbance peaks at 420 nm. In addition, it agrees with the findings of Vijaya et al. (2017) and Singh et al. (2017), who also found that Ag-NPs produced from dried root suspension of *Zingiber officinale* exhibited a single symmetric peak at 425 nm [72, 73].

There was no significant difference in the SPR of evaluation for each monthly UV examination of the colloidal AgNPs sample, demonstrating high stability against agglomeration. After three months in the fridge at 4°C, the sample showed no signs of degradation

4.4.2 AFM image of synthesized AgNPs

The majority of the NPs in our investigation had a spherical form, as shown in the AFM images. Compared to the results obtained from DLS measurements (119.80 ± 1.7 nm), the lesser diameter (40 to 80 nm) was observed. This occurred as a result of the Brownian motion of the nanoparticles inside the colloidal system. Light scattering as a function of particle size via colloidal particles is measured by DLS in this condition [74]. Alternatively, AFM analysis involved precisely measuring the height of each nanoparticle [75]. This finding aligns with a study that utilized clove and eugenol for the synthesis of AgNPs, where the DLS results indicated an average size of (55.4 ± 4.1 nm and 57.4 ± 0.2 nm) for the AgNPs derived from clove and eugenol, respectively. The results from Transmission Electron Microscopy (TEM) indicated sizes of 45.6 ± 6.1 nm for clove AgNPs and 40.4 ± 5.3 nm for eugenol AgNPs [69].

4.4.3 DLS and Zeta Potential Analysis for Synthesized AgNPs

DLS is a technique that quantifies the nanoparticle's hydrodynamic diameter, exhibiting Brownian motion inside a colloidal sample. The approach is utilized to ascertain the intensity variations of dispersed light within the sample. The diffusion coefficient of the particles is determined by examining the intensity of the observed scattered light. The Stokes-Einstein equation is employed to determine the hydrodynamic diameter [76]. Information regarding the size distribution and stability of the colloidal systems is provided by DLS analysis [77]. Furthermore, nanoparticle surface charges may be quantified using zeta potential. The particles are strongly electrostatically repelled from one another, which prevents them from aggregating and increases their stability, as indicated by the high zeta potential value. When the zeta potential is more than 30 mV or less than -30 mV, researchers state that the colloidal solution is stable [76]. In Pharmaceutics, a colloidal system must be stable to ensure consistent therapeutic effects and prevent aggregation. The combination of DLS and zeta potential analysis will achieve these properties.

In our study, the average effective diameter by DLS measuring was (119.80 ±1.7 nm), this value is higher than the one obtained by AFM analysis (40-80 nm) as mentioned above because of the Brownian motion of particles in a colloidal sample. In other words, the hydrodynamic radius is the total of the actual diameter plus the surrounding layers,

not the size of the particle. The technique determines the hydrodynamic size of particles by measuring the light scattered from a laser that passes through the colloidal particles [74]. This result goes along with the results of a previous study done by Al Sharif and others 2020, they synthesized AgNPs using *Bacillus, the diameter of which its diameter* obtained by TEM (6–50nm,) was smaller than the DLS measurement for the same NP (82.01 nm) [78]. As the diameter of nanoparticles decreased, the biological activity increased, smaller particle sizes increase surface area, which indicates more interaction between particles and microorganisms.

The polydispersity index was determined to be 0.220 ± 0.04, indicating that the particles exhibited uniform size. This aligns with the findings from the AFM morphological analysis [79].

The zeta potential value measured at -43.86 ±2.2 mV suggests a stable colloidal sample. Nonetheless, the chemical interactions between the phytochemicals present in the essential oil and the nanoparticle surfaces could facilitate steric stabilization.

4.4.5 Antioxidant Evaluation of Synthesized AgNPs and *T. capitatus* EO

DPPH is a free radical that is used to evaluate the antioxidant activity of different chemical compounds. This assessment technique established if the molecule might serve as an electron or hydrogen donor in the conversion of DPPH into its reduced form, DPPH is stable and has a purple solution, the principle of anti-oxidant assessment depends on the conversion of DPPH solutions' color from pale yellow, which means the disappearance of the maximum absorbance that occurs at 517 nm using UV-visible spectroscopy. When a chemical has anti-oxidant properties the DPPH is decreased [58].

This study demonstrated that produced AgNPs had a strong antioxidant activity by scavenging free radicals. Concentrations ranging from 0 to 100 µg/mL had an impact that was dose-dependent, meaning that the antioxidant activity of the produced AgNPs increased as the concentrations rose. This finding is in agreement with what Melkamu et al. found in their investigation. In 2021, the researchers isolated AgNPs from the leaves of the Hagenia abyssinica (Bruce) J.F. Gmel plant and discovered that the nanoparticles' antioxidant properties improved as the concentration increased (10 µg/mL-320 µg/mL) [80].

Moreover, Hana Bajes and Sawsan Oran (2023) studied the antioxidant activity of *T. capitatus* pure oil using a DPPH assay; they reported that *T. capitatus* oil has significant anti-oxidant properties and its potency was concentration-dependent. The positive control was ascorbic acid with an IC_{50} value of 4.1 µg/ml, whereas *T. capitatus* oil had an IC_{50} of 6.4 µg/ml, which means it exhibits a high antioxidant activity [81].

In our study IC_{50} values for Trolox, synthesized AgNPs, *T. capitatus* pure oil were (2.27 ±0.91, 10.47 ±1.11 µg/ml, and 48.97 ±1.20 µg/ml) respectively. The maximum tested concentration of AgNPs (100 µg/ml) exhibited the highest anti-oxidant activity (nearly 95% inhibition), which was near the inhibition percent of the Trolox at the same tested concentration.

Compared to the pure oil of *T. capitatus*, the antioxidant activity of synthesized AgNPs was about 5-fold greater than that of pure oil, this is due to the combination of phenolic compounds in the oil with silver ions which increase the anti-scavenger effect.

Several studies approved those nanoparticles loaded with an essential oil had a more potent anti-oxidant activity than the essential oil itself. Sambhakar et al. (2023) created a nanoemulsion of pomegranate seed oil exhibiting superior antioxidant activity compared to the oil in its original form. This boost pertains to the enhanced solubilization capacity of the nanoemulsion, which exceeds that of oil and other pharmaceutical formulations, attributable to the nanoemulsion's much greater surface area and its very tiny particle size.

Another study done by Wang et al. (2023) explored the beneficial properties of lingonberry leaf extract and its active compounds when formulated as a nanoemulsion. The nanoemulsions demonstrated enhanced antioxidant activity, inhibiting DPPH radicals by over 13% more effectively than their non-nanoemulsified extract. The differences were statistically significant. That was due to the encapsulation of polyphenols in nanoscale emulsions significantly boosting their solubility, thereby optimizing their antioxidant potential.

This suggests that nanoemulsion technology is crucial in enhancing the bioavailability and therapeutic efficacy of natural compounds, such as polyphenols, by improving their solubility and stability, leading to more effective biological activities. [82]

4.5 Anti-Microbial Assay

The antimicrobial resistance property of many microorganisms is posing a serious life-threatening problem worldwide [34]. However, several herbal EOs have excellent anti-microbial activity against bacteria, viruses, parasites, and fungi. This antimicrobial activity is due to the presence of different compounds [33, 34, 83]. *T. capitatus* is recognized as a medicinal plant; previous investigations have demonstrated that the oil exhibits efficacy against both Gram-positive and Gram-negative bacteria, as well as *Candida albicans*. The presence of phenolic compounds such as carvacrol and thymol may inhibit enzymes that play a role in cell wall synthesis. Additionally, γ-terpinène and p-cymene have been documented to exhibit antifungal activity [10, 11].

It was reported that the effectiveness of *T. capitatus* EO and synthesized AgNPs may be due to the phenolic compounds and silver ion release, respectively, which may interact with enzymes such as chitinase, chitin synthase, α, and ß-glucanases, which are involved in fungal cell wall synthesis [33, 61].

The mechanism by which AgNPs exhibit antibacterial activity is currently under investigation. It is possible that the presence of silver ions interacts with the thiol and sulfhydryl groups present in the protein of the bacterial cell membrane, resulting in damage to the cellular respiratory system and ultimately leading to cell death. Another theory suggests that AgNPs may bind to DNA and RNA via the cell membrane, thereby inhibiting replication and causing denaturation [84].

In this research, the MIC of synthesized AgNPs and *T. capitatus* EO was determined using the broth microdilution method, and turbidity was utilized to measure the growth of bacteria in the microplate wells. Both *T. capitatus* EO and its synthesized AgNPs had significant antimicrobial activity. MIC values for synthesized AgNPs were between 0.130 ±0.001 µg/ml and 0.290 ±0.004 µg/ml against the bacteria strains tested and 0.016 ±0.00 µg/ml for *candida albicans*. Whereas MIC values of the oil range between (0.625 ± 0.002 µg/ml and 1.562 ±0.004 µg/ml) against six types of most common bacterial strains and (0.078 ±0.00 µg/ml) against *Candida albicans*.

These results confirm that the synthesized AgNPs are more potent than *T. capitatus* EO as an antibacterial agent, nearly 5 folds. This potency is due to the presence of silver ions that are attracted to the negative charge of the bacterial cell wall, this electrostatic

attraction will affect the cell wall permeability by changing its composition, leading to the leakage of cell components and cell death [84, 85]. Furthermore, other studies reported that the contact area between nanosized particles and the surface of microorganisms is greater than the interaction with larger particles, as a result, the anti-microbial activity of NPs is consequently higher. Another important result is the efficiency of excellent activity of both *T. capitatus* EO and synthesized AgNPs against the MRSA strain, which is resistant to most antibiotics.

The antimicrobial activity of synthesized nanoparticles is derived from a combination of the pure oil and silver ion action. The pure oil has a potent antimicrobial effect, and the release of silver ions interacts with the cell membrane and damages it. An important rule is that the smaller nanoparticles increase the surface area of nanoparticles at the site of action, which improves their activity.

Our results go along with other studies which confirmed the anti-microbial potency of AgNPs. Going back to the literature, Küp FÖ, Çoşkunçay S, and Duman F (2020) synthesized AgNPs with Aesculus hippocastanum leaf extracts and evaluated their antibacterial efficacy. The results demonstrated that whereas AgNPs lacked antifungal properties, they exhibited potent antibacterial activity against several Gram-positive and Gram-negative bacterial species [86] However, other studies have discovered that green-produced AgNPs have strong antifungal effects against some fungi. AgNPs were created by Jyoti Singh, Ankit Kumar, and colleagues using leaf extract from Azadirachta indica, and their antifungal efficacy against four distinct fungal species was evaluated. The synthesized AgNP exhibited an inhibition range of 68% to 80% against Rhizoctonia solani and Colletotrichum gloeosporioides at a concentration of 2000 ppm, achieving complete inhibition against Sclerotinia sclerotiorum and Colletotrichum falcatum [87]. Silver nanoparticles have the potential to address the difficulties associated with the penetration of medical agents through fungal cell walls. The most recent findings indicate that while the material is durable and rugged, green-synthesized AgNPs have demonstrated the ability to decompose the fungal cell wall by inhibiting the proton pump and releasing reactive oxygen species. Furthermore, it is proposed that the swift introduction of AgNPs causes a rise in the outflow of intracellular ions; consequently, this damages the respiratory system, leading to cell death [88].

4.6 Cytotoxicity assay for *T. capitatus* EO and synthesized AgNPs

Cytotoxicity assay provides information on the interaction between cells and toxic compounds, as well as their metabolism, survival, and death. The anticancer activity of *T. capitatus* EO has been extensively studied. Carvacrol, p-cymene, terpinene, and thymol are the major chemical constituents that give biological activity [2, 11, 12].

Recent studies have been conducted to investigate the mechanisms underlying AgNP cytotoxicity, focusing on identifying the primary cause of cell death: whether it is due to the AgNPs themselves or the Ag ions released from the nanoparticles. The production of reactive oxygen species (ROS), which triggers oxidative stress and leads to cell death, is often dependent on silver ions [89]. Additional research indicates that lysosomal entrapment is essential for increased Ag ion release. However; it has been reported that the cytotoxicity of AgNPs relies on the nanoparticles themselves depending on the uptake efficiency. Endocytosis is the main drive mechanism for AgNPs to be taken up by the cells [90]. Additionally, electron microscopy confirms that AgNPs are contained in endocytic vesicles, lending credence to this theory.

However, in some cancer cells, there were alternative uptake mechanisms because of the impairment of endocytotic pathways. Furthermore, endocytosis doesn't have the same NPs uptake efficiency in all cell types. For example, it has been observed that glucose- and lactose-capped AgNPs are internalized in a similar manner by L929 fibroblast cells, while A549 carcinoma cells exhibit a greater uptake efficiency for lactose-modified AgNPs compared to glucose-modified AgNPs [91].

This study employed the MTS assay to assess the toxicity of synthesized AgNPs and *T. capitatus* EO on various cell lines, including cervical cancer cells (HeLa), breast cancer cells (MCF-7), fibroblast cells derived from mouse embryos (3T3), human embryonic kidney cells (HEK293), human hepatocellular carcinoma cells (Hep-3B), and melanoma cells isolated from mouse skin (B16F1). The findings shown that both EO and manufactured AgNPs have significant cytotoxic efficacy against all used cell lines. The cytotoxicity escalated with an increase in concentration. Nonetheless, manufactured AgNPs exhibited more toxicity than the essential oil. The cytotoxic activity of synthesized nanoparticles is derived from a combination of the pure oil and silver ion action. Pure oil has a great cytotoxic effect, and the release of silver ions generates ROS,

resulting in damage to the mitochondria and DNA of cancer cells. Furthermore, the smaller nanoparticles increase the surface area of nanoparticles at the site of action, which improves their activity.

The IC_{50} values for the synthesized AgNPs and *T. capitatus* EO against HeLa cells were (25.11±0.5 and 38.9 ±0.5 µg/ml), respectively. While against MCF-7 celles were (22.9 ±0.5 and 33.41 ±0.5 µg/ml) respectively. Against 3T3 cells were (18.19 ±0.5 and 27.54 ±0.5 µg/ml) respectively. Against HEK293 were (18.19 ±0.5 and 21.87 ±0.5 µg/ml) respectively. Against Hep-3B cells were (22.38 ±0.5 and 31.62 ±0.5 µg/ml) respectively. And against B16-F1 were (27.54 ±0.5, 33.65 ±0.5 µg/ml). Comparing these IC_{50} values to the positive control, doxorubicin which had IC_{50} values of (10.11 ±1.17 µg/ml) against HeLa, (15.02 ±0.72 µg/ml) against MCF-7 [92], (3.243 µg/ml) against NIH3T3 [93], (2 µg/ml) against HEK293 [94], (0.773 µg/ml) against B16-F1 [95], and (21.37 ±0.63 µg/ml) against Hep-3B [92]. Our result reveals that the anti-cancer potency of synthesized AgNPs against hepatocellular carcinoma (Hep-3B) is nearly the same potency of doxorubicin IC_{50} values (22.38 µg/ml, 21.37 µg/ml) respectively.

The findings align with those reported by Gomathi AC, Xavier Rajarathinam SR et al. (2020), who successfully synthesized AgNPs from tamarind fruit shells. The synthesized AgNPs demonstrated significant anti-cancer activity against human breast cancer cells (MCF-7 cell lines). The apoptotic action exhibited a dose-dependent relationship, with an inhibitory concentration (IC_{50}) measured at 20 µg/ml. It has been reported that NP-generated ROS resulted in damage to the mitochondria and DNA of cancer cells [96]. Additionally, another study demonstrated that AgNPs induce autophagy in breast cancer cells. Gopisetty MK et al. (2019) demonstrated that 75 nm AgNPs markedly decreased Pgp efflux activity in drug-resistant breast cancer cells and amplified the apoptotic effect induced by doxorubicin. The study revealed that AgNPs reduced the calcium levels stored in the endoplasmic reticulum (ER), induced stress within the ER, and compromised the integrity of the Pgp plasma membrane [97].

Bakrania A, Zheng G, and Bhat M (2022) indicated that silver nanoparticles enhance the treatment of hepatocellular carcinoma, as traditional therapies often fall short, by improving drug bioavailability and minimizing adverse effects on healthy cells [98].

4.7 Anti-Inflammatory Evaluation of Synthesized AgNPs and *T. capitatus* EO

Inflammation occurs when the immune system activates and produces anti-inflammatory mediators like cytokines, chemokines, tumor necrosis factor-α, and enzymes like cyclooxygenase-1 (COX-1) and cyclooxygenase-2 (COX-2) [99]. Inflammation is now known to be linked to several illnesses, including high blood pressure, heart disease, lung conditions like asthma, Alzheimer's disease, type 2 diabetes, gastrointestinal disorders like Crohn's disease and ulcerative colitis, autoimmune diseases like rheumatoid arthritis, and some types of cancer [100].

Nonsteroidal anti-inflammatory drugs (NSAIDs), glucocorticoids, and immunosuppressants were identified as anti-inflammatory medications. Nonetheless, given the various adverse side effects linked to these treatments, it is essential to investigate safer alternatives. The mechanism underlying the anti-inflammatory effect of the produced AgNPs remains unclear. In vitro studies indicate that the generated AgNPs have the potential to suppress the production of pro-inflammatory cytokines, including TNF-α and COX-2 isozyme [99]. Nanoparticles (NPs) are thought to be more effective anti-inflammatory agents than bulk samples due to their high surface area to volume ratio.

This study investigates the possible anti-inflammatory effects of synthesized AgNPs and *T. capitatus* EO on COX-1 and COX-2 isozymes. The potency (IC_{50} values) of both pure oil and synthesized AgNPs towards COX-1 were found to be 23.7 µg/mL and 7.71 µg/mL, respectively, in comparison to the positive control ketoprofen, which had an IC_{50} value of 7.89 µg/mL. The IC_{50} values for both pure oil and AgNPs against COX-2 were found to be 19.42 µg/mL and 2.83 µg/mL, respectively, in comparison to ketoprofen, which had an IC_{50} value of 40.18 µg/mL. Among the tested samples, synthesized AgNPs exhibited the highest inhibitory effect on COX-2, achieving an IC_{50} value of 2.83 µg/mL, which is 14% of the ketoprofen IC_{50} value of 40.18 µg/mL. Additionally, synthesized AgNPs demonstrated comparable activity to ketoprofen against COX-1, with IC_{50} values of 7.71 µg/mL and 7.89 µg/mL, respectively. The IC_{50} value of *T. capitatus* pure oil (19.42) for COX-2 indicates that it is (50%) of the IC_{50} of ketoprofen.

This study is the first to assess the anti-inflammatory properties of green-synthesized silver nanoparticles using *T. capitatus* essential oil, as indicated by the available literature review. Nevertheless, the anti-inflammatory potential of green-synthesized AgNPs has not been extensively investigated by researchers. Yang B, Dong Y, Wang F, and Zhang

Y (2020) demonstrated that silver nanoparticles synthesized from aqueous leaf extract of Clinacanthus nutans possess analgesic and muscle-relaxant properties [101].

Seethalakshmi S AMKM published that AgNPs-synthesized *Piper nigrum* extract had selective inhibitory action towards cytokines IL-1β and IL-6 [102]. Furthermore, in 2023, Khashan AA, Dawood Y, and Khalaf YH demonstrated that in arthritic Wistar rats, AgNPs from Viburnum opulus fruit extract decreased plasmatic IL-6 levels [103] These studies have revealed that plant chemical constituents (phenols, terpinoides, flavanoides, and tannins) have anti-inflammatory activity. It is believed that their anti-inflammatory properties result from inhibiting enzymes involved in the production of the chemical mediators of inflammation [65].

Finally, the biological activity of manufactured nanoparticles is derived from the combination of the pure oil and silver ion effects. Furthermore, the smaller nanoparticles increase the surface area of nanoparticles at the site of action, enhancing their activity.

4.8 Limitations of Green Synthesis of AgNPs

Despite the advantages of green synthesis of silver nanoparticles, there are a few limitations that need further investigation. The first of all is the variation in chemical constituents of the plant extract. This challenge affects the method of synthesis and also pla ys a crucial role in the physiochemical properties of the synthesized AgNPs and their stability. In addition, several factors affect the synthesis procedure such as the concentration of silver ions precursor, temperature, pH, and reaction time. Another limitation is the *in vivo* cytotoxicity assessment of synthesized AgNPs on normal healthy cells.

In this work the most important challenge was the determination of the optimal parameters for the optimal synthesis of AgNPs, several trials were applied, and finally, we had the most appropriate method for synthesis.

Therefore, several studies must be done on the same plant genus to develop the most appropriate synthesis method with consistent parameters, yielding highly consistent, effective nanoparticles for their promising application as antibacterial, antifungal, and anticancer agents in many medicinal fields. In addition, further studies are needed on AgNP cytotoxicity on healthy normal cell lines.

4.9 Conclusion

This thesis evaluates the potential for green synthesis of silver nanoparticles utilizing *T. capitatus* essential oil and optimizes its biological activities. The *T. capitatus* plant was collected from various regions of Palestine and underwent hydrodistillation extraction. The essential oil constituents were identified and separated using GC-MS analysis. The major compounds included Carvacrol (37.47%), P-cymene (27.96%), and γ-Terpinene (26.3%). The EO was effectively utilized in the green synthesis of AgNPs. A 0.1 M solution of silver nitrate (AgNO=3) served as the precursor for silver ions. The optimal synthesis was achieved by identifying the ideal parameters while gradually adding diluted EO to the AgNO=3 solution under moderate magnetic stirring. The initial observation of nanoparticle formation was indicated by a color change to dark brown.
The colloidal sample of AgNPs was characterized by several analyzers, including a UV–visible spectrometer, AFM, DLS, and a zeta potential analyzer. The UV-visible analysis validated the nucleation of nanoparticles, yielding a spectral peak at 423 nm. AFM analysis showed that AgNPs were spherical and ranged in size from 40 to 80 nm; this diameter range was less than that obtained by DLS, which was 119.80 ± 1.7 nm, and the zeta potential value was -43.86 ± 2.2.

n vitro tests were conducted to assess the biological activity of synthesized AgNPs in comparison to pure oil. The DPPH assay measured antioxidant activity. The synthesized AgNPs exhibited a potency five times greater than that of pure *T. capitatus* oil, with IC_{50} values recorded as 2.27 ± 0.91 μg/ml for Trolox, 10.47 ± 1.11 μg/ml for synthesized AgNPs, and 48.97 ± 1.20 μg/ml for *T. capitatus* oil.

Antimicrobial activity was assessed using the broth microdilution method, and results showed that synthesized AgNPs presented antimicrobial activity about 5-fold greater than *T. capitatus* pure oil against all bacterial strains that were used in addition *to candida albicans*, with MIC values ranging between (0.016 ± 0.00 μg/ml, 0.290 ± 0.004 μg/ml) for AgNPs, and (0.078 ± 0.00 μg/ml and 1.562 ± 0.004 μg/ml) for pure *T. capitatus* EO. Cytotoxic activity was assessed on different cell lines including; HeLa, MCF-7, NIH 3T3, HEK293, Hep-3B, and B16F1 cell., The results revealed that EO and synthesized AgNPs have great cytotoxic activity against all used cell lines, compared to doxorubicin. The percent of inhibition of synthesized NP was nearly 80% at concentrations around 200 μg/mL. The IC_{50} values for the synthesized AgNPs and *T. capitatus* EO against HeLa cells

were 25.11 ± 0.5 μg/ml and 38.9 ± 0.5 μg/ml, respectively. The values against MCF-7 cells were 22.9 ±0.5 and 33.41 ±0.5 μg/mL, respectively. In relation to 3T3 cells, the values were 18.19 ± 0.5 and 27.54 ± 0.5 μg/ml, respectively. The values against HEK293 were 18.19 ±0.5 and 21.87 ±0.5 μg/ml, respectively. The values against Hep-3B cells were 22.38 ±0.5 and 31.62 ±0.5 μg/ml, respectively. The measurements against B16-F1 were (27.54 ±0.5, 33.65 ±0.5 μg/ml). Synthesized AgNPs exhibited the highest inhibitory effect on COX-2, with an IC_{50} value of 2.83 μg/mL, corresponding to 14% of the ketoprofen IC_{50} value of 40.18 μg/mL.

Finally, the available literature survey reveals a significant number of publications on the green synthesis of AgNPs using plant extract, and this number continues to rise annually. This study represents the first work that assesses the antibacterial, anticancer, antioxidant, and anti-inflammatory activities of synthesized AgNPs using Palestinian *T. capitatus* EO. Overall, previous results have suggested a potential new biomedical agent that could be used in various treatment therapies to enhance effectiveness and reduce side effects, particularly in cancer treatment. Furthermore, we advocate combining the synthesized nanoparticles into a topical formulation and subjecting it to in vitro and in vivo experiments to determine its biological activity as a treatment for various skin problems, such as wound healing, burns, and cellulitis.

List of Abbreviations

Abbreviation	Meaning
AgNPs	Silver Nanoparticles
$AgNO_3$	Silver Nitrates
ATCC	American Type Culture Collection
C	Degree Celsius
DMSO	Dimethyl sulfoxide
E. coli	Escherichia coli
EO	Essential Oil
GC-MS	Gas Chromatography-Mass Spectrometry
g	Gram
Hep-G2	Hepatic G2
K. pneumonia	Klebsiella pneumonia
L	Letter
M	Molarity
MCF-7	Human Breast Cancer Cell
mcg	Microgram
MIC	Minimum inhibitory concentration
min	Minute
ml	Milliliter
RBMI	Roswell Park Memorial Institute Medium
T. capitatus	Thymus capitatus
UV	Ultraviolet
(w/w)	Weight by weight
NPs	Nanoparticles

References

1. Bolouri P, Salami R, Kouhi S, Kordi M, Asgari Lajayer B, Hadian J, Astatkie T: **Applications of Essential Oils and Plant Extracts in Different Industries**. *Molecules* 2022, **27**(24):8999.

2. Ramos da Silva LR, Ferreira OO, Cruz JN, de Jesus Pereira Franco C ,Oliveira dos Anjos T, Cascaes MM, Almeida da Costa W, Helena de Aguiar Andrade E, Santana de Oliveira M, Luís Â: **Lamiaceae Essential Oils, Phytochemical Profile, Antioxidant, and Biological Activities**. *Evidence-Based Complementary and Alternative Medicine* 2021, **2021**:1-18.

3. Sinan KI, Etienne OK, Stefanucci A, Mollica A, Mahomoodally MF, Jugreet S, Rocchetti G, Lucini L, Aktumsek A, Montesano D *et al*: **Chemodiversity and biological activity of essential oils from three species from the Euphorbia genus**. *Flavour and Fragrance Journal* 2020, **36**(1):148-158.

4. Parupudi A, Mulagapati SHR, Subramony JA: **Chapter 1 - Nanoparticle technologies: Recent state of the art and emerging opportunities**. In: *Nanoparticle Therapeutics.* Edited by Kesharwani P, Singh KK: Academic Press; 2022: 3-46.

5. Asif M, Yasmin R: **Green Synthesis of Silver Nanoparticles (AgNPs), Structural Characterization, and their Antibacterial Potential**. *Dose Response* ,2022 .15593258221088709:(1)20

6 . Tongnuanchan P, Benjakul S (2014): **Essential oils: extraction, bioactivities, and their uses for food preservation.** *J Food Sci*, 79(7):R1231-1249.

.7 Sehnal, Hosnedlova, Docekalova, Stankova, Uhlirova, Tothova, Kepinska, Milnerowicz, Fernandez, Ruttkay N *et al*: **An Assessment of the Effect of Green Synthesized Silver Nanoparticles Using Sage Leaves (Salvia officinalis L.) on Germinated Plants of Maize (Zea mays L.)**. *Nanomaterials* 2019, **9**(11):1550.

.8 Tagnaout I, Zerkani H, Hadi N, El Moumen B, El Makhoukhi F, Bouhrim M, Al-Salahi R, Nasr FA, Mechchate H, Zair T: **Chemical Composition, Antioxidant and Antibacterial Activities of Thymus broussonetii Boiss and Thymus capitatus (L.) Hoffmann and Link Essential Oils**. *Plants* 2022, **11**(7):954.

.9 Zaïri A, Nouir S, Zarrouk A, Haddad H, Khélifa A, Achour L, Tangy F ,Chaouachi M, Trabelsi M: **Chemical composition, Fatty acids profile and Biological properties of Thymus capitatus (L.) Hoffmanns, essential Oil**. *Scientific Reports* 2019, **9**(1):20134.

.10 Gonçalves JC, de Meneses DA, de Vasconcelos AP, Piauilino CA, Almeida FR, Napoli EM, Ruberto G, de Araújo DA: **Essential oil composition and antinociceptive activity of Thymus capitatus**. *Pharm Biol* 2017, **55**(1):782-786.

.11 Goudjil MB, Zighmi S, Hamada D, Mahcene Z, Bencheikh SE, Ladjel S: **Biological activities of essential oils extracted from Thymus capitatus (Lamiaceae)**. *South African Journal of Botany* 2020, **128**:274-282.

.12 Mohamed Bilal Goudjil, Souad Zighmi, Hamada D, ZM, Salah Eddine Bencheikh,, Ladjel S: **Biological activities of essential oils extracted from Thymus capitatus (Lamiaceae)**. *South African Journal of Botany* 2020, **128**:274-282.

.13 Benoutman A, Erbiai EH, Edderdaki FZ, Cherif EK, Saidi R, Lamrani Z, Pintado M, Pinto E, Esteves da Silva JCG, Maouni A: **Phytochemical Composition, Antioxidant and Antifungal Activity of Thymus capitatus, a Medicinal Plant Collected from Northern Morocco**. *Antibiotics (Basel)* 2022, **11**.(5)

.14 Bounatirou S, Smiti S, Miguel M, Faleiro L, Rejeb M, Neffati M, Costa M, Figueiredo A, Barroso J, Pedro L: **Chemical composition, antioxidant and antibacterial activities of the essential oils isolated from Tunisian Thymus capitatus Hoff. et Link**. *Food Chemistry* 2007, **105**(1):146-155.

.15 Aissaoui AB, Amrani AE, Zantar S, Toukour L: **Activité Acaricide Des Huiles Essentielles Du Mentha Pulegium ,Origanum Compactum Et Thymus Capitatus Sur L'acarien Phytophage Tetranychus Urticae Koch (Acari: Tetranychidae)**. *European Scientific Journal* 2018, **14**.(3)

.16 Chee PL, Toh WL, Yew PY, Peng S, Kai D: **Introduction of Nanotechnology and Sustainability**. In: *Sustainable Nanotechnology.* Edited by Li Z, Zheng J, Ye E: The Royal Society of Chemistry; 2022: 0.

.17 Toumey C: **Plenty of room, plenty of history**. *Nature Nanotechnology* 2009, **4**(12):783-784.

.18 Bayda S, Adeel M, Tuccinardi T: **The History of Nanoscience and Nanotechnology: From Chemical-Physical Applications to Nanomedicine**. 2019, **25**.(1)

.19 Anirban A: **40 years of scanning tunnelling microscopy**. *Nature Reviews Physics* 2022, **4**(5):291-291.

.20 Haleem A, Javaid M, Singh RP, Rab S, Suman R: **Applications of nanotechnology in medical field: a brief review**. *Global Health Journal* 2023, **7**(2):70-77.

.21 Dang Y, Guan J: **Nanoparticle-based drug delivery systems for cancer therapy**. *Smart Materials in Medicine* 2020, **1**:10-19.

.22 Xia Y, Sun J, Zhao L, Zhang F, Liang X-J ,Guo Y, Weir MD, Reynolds MA, Gu N, Xu HHK: **Magnetic field and nano-scaffolds with stem cells to enhance bone regeneration**. *Biomaterials* 2018, **183**:151-170.

.23 Lee DH, Lee SH, Kim AR, Quan FS: **Virus-Like Nanoparticle Vaccine Confers Protection against Toxoplasma gondii**. *PloS one* 2016, **11**(8):e0161231.

.24 Zhang C, Yan L, Wang X, Zhu S, Chen C, Gu Z, Zhao Y: **Progress, challenges, and future of nanomedicine**. *Nano Today* 2020, **35**:101008.

.25 Rizwan M, Shoukat A, Ayub A, Razzaq B, Tahir MB: **Nanomaterials: Synthesis, Characterization, Hazards and Safety Chpter 3**. In: *Nanomaterials: Synthesis, Characterization, Hazards and Safety.* Edited by Tahir MB, Sagir M, Asiri AM: Elsevier; 2021: 31-54.

.26 Bruna T, Maldonado-Bravo F, Jara P, Caro N: **Silver Nanoparticles and Their Antibacterial Applications**. *International journal of molecular sciences* 2021, **22**(13):7202.

.27 Manring MM, Hawk A, Calhoun JH, Andersen RC: **Treatment of war wounds: a historical review**. *Clinical orthopaedics and related research* 2009, **467**(8):2168-.2191

.28 Khansa I, Schoenbrunner AR, Kraft CT, Janis JE: **Silver in Wound Care-Friend or Foe?: A Comprehensive Review**. *Plastic and reconstructive surgery Global open* 2019, **7**(8):e2390.

.29 Corsi I, Desimone MF, Cazenave J: **Building the Bridge From Aquatic Nanotoxicology to Safety by Design Silver Nanoparticles**. *Frontiers in Bioengineering and Biotechnology* 2022, **10**.

.30 Zhang XF, Liu ZG, Shen W, Gurunathan S: **Silver Nanoparticles: Synthesis, Characterization, Properties, Applications, and Therapeutic Approaches**. *International journal of molecular sciences* 2016, **17**(9):1534.

.31 Xu L, Wang YY, Huang J, Chen CY, Wang ZX, Xie H: **Silver nanoparticles: Synthesis, medical applications and biosafety**. *Theranostics* 2020, **10**(20):8996-9031.

.32 Szczyglewska P, Feliczak-Guzik A, Nowak I: **Nanotechnology–General Aspects: A Chemical Reduction Approach to the Synthesis of Nanoparticles**. *Molecules* 2023, **28**(13):4932.

.33 Islam MA, Jacob MV, Antunes E: **A critical review on silver nanoparticles: From synthesis and applications to its mitigation through low-cost adsorption by biochar**. *Journal of Environmental Management* 2021, **281**:111918.

.34 Dhaka A, Chand Mali S, Sharma S, Trivedi R: **A review on biological synthesis of silver nanoparticles and their potential applications**. *Results in Chemistry* 2023, **6**:101108.

.35 Mallikarjuna K, John Sushma N, Narasimha G, Manoj L, Deva Prasad Raju B: **Phytochemical fabrication and characterization of silver nanoparticles by using Pepper leaf broth**. *Arabian Journal of Chemistry* 2014, **7**(6):1099.1103-

.36 Giri AK, Jena B, Biswal B, Pradhan AK, Arakha M, Acharya S, Acharya L: **Green synthesis and characterization of silver nanoparticles using Eugenia roxburghii DC. extract and activity against biofilm-producing bacteria**. *Scientific Reports* 2022, **12**.8383:(1)

.37 Hazarika D, Phukan A, Saikia E, Chetia B: **Phytochemical screening and synthesis of silver nanoparticles using leaf extract of Rhynchotechum ellipticum**. *International Journal of Pharmacy and Pharmaceutical Sciences* 2014, **6**:672-674.

.38 Ahmad S, Munir S, Zeb N, Ullah A, Khan B, Ali J, Bilal M, Omer M, Alamzeb M, Salman SM *et al*: **<p>Green nanotechnology: a review on green synthesis of silver**

nanoparticles — an ecofriendly approach</p>. *International Journal of Nanomedicine* 2019, **Volume 14**:5087.5107-

.39 Akhter MS, Rahman MA, Ripon RK, Mubarak M, Akter M, Mahbub S, Al Mamun F, Sikder MT: **A systematic review on green synthesis of silver nanoparticles using plants extract and their bio-medical applications**. *Heliyon* 2024, **10**(11):e29766.

.40 Antunes Filho S, Dos Santos MS: **Biosnnynthesis of Nanoparticles Using Plant Extracts and Essential Oils**. 2023, **28**.(7)

.41 Alharbi NS, Alsubhi NS, Felimban AI: **Green synthesis of silver nanoparticles using medicinal plants: Characterization and application**. *Journal of Radiation Research and Applied Sciences* 2022, **15**(3):109-124.

.42 Arshad F, Naikoo GA, Hassan IU, Chava SR, El-Tanani M, Aljabali AA, Tambuwala MM: **Bioinspired and Green Synthesis of Silver Nanoparticles for Medical Applications: A Green Perspective** .*Applied Biochemistry and Biotechnology* 2024, **196**(6):3636-3669.

.43 Akbarzadeh A, Kafshdooz L, Razban Z, Dastranj Tbrizi A, Rasoulpour S, Khalilov R, Kavetskyy T, Saghfi S, Nasibova AN, Kaamyabi S *et al*: **An overview application of silver nanoparticles in inhibition of herpes simplex virus**. *Artificial Cells, Nanomedicine, and Biotechnology* 2018, **46**(2):263-267.

.44 Bray F, Laversanne M, Sung H, Ferlay J, Siegel RL, Soerjomataram I, Jemal A: **Global cancer statistics 2022: GLOBOCAN estimates of incidence and mortality worldwide for 36 cancers in 185 countries**. *CA: A Cancer Journal for Clinicians* 2024, **74**(3):229-263.

.45 Kovács D, Igaz N, Gopisetty MK, Kiricsi M: **Cancer Therapy by Silver Nanoparticles: Fiction or Reality?** *International journal of molecular sciences* 2022, **23**.(2)

.46 Ovais M, Khalil AT, Raza A, Khan MA, Ahmad I, Islam NU, Saravanan M, Ubaid MF, Ali M, Shinwari ZK: **Green Synthesis of Silver Nanoparticles Via Plant Extracts: Beginning a New Era in Cancer Theranostics**. *Nanomedicine* 2016, **11**(23):315.3177-7

.47 Bustamante J, van Stempvoort S, García-Gallarreta M, Houghton JA, Briers HK, Budarin VL, Matharu AS, Clark JH: **Microwave assisted hydro-distillation of essential oils from wet citrus peel waste**. *Journal of Cleaner Production* 2016, **137**:598-605.

.48 G. W. A. Milne WLB, S. R. Heller, D. P. Martinsen, R. G. Oldham: **Quality control and evaluation of mass spectra**. *Organic Mass Spectrometry* 1982, **17**(11):547-552.

.49 Jaradat N, Al-Maharik N, Abdallah S, Shawahna R, Mousa A, Qtishat A: **Nepeta curviflora essential oil: Phytochemical composition, antioxidant, anti-proliferative and anti-migratory efficacy against cervical cancer cells, and α-glucosidase, α-amylase and porcine pancreatic lipase inhibitory activities**. *Industrial Crops and Products* 2020, **15**.8:112946

.50 Ahmad K, Asif HM, Afzal T, Khan MA, Younus M, Khurshid U, Safdar M, Saifulah S, Ahmad B, Sufyan A *et al*: **Green synthesis and characterization of silver nanoparticles through the Piper cubeba ethanolic extract and their enzyme inhibitory activities**. *Frontiers in Chemistry* 2023, **11**.

.51 Zhang XF, Liu ZG, Shen W, Gurunathan S: **Silver Nanoparticles: Synthesis, Characterization, Properties, Applications, and Therapeutic Approaches**. *International journal of molecular sciences* 2016, **17**.(9)

.52 Sawalha S, Abdallah S, Barham A, Badawi H, Barham Z, Ghareeb A, Misia G, Collavini S, Silvestri A, Prato M *et al*: **Green synthesis of fluorescent carbon nanodots from sage leaves for selective anticancer activity on 2D liver cancer cells and 3D multicellular tumor spheroids**. *Nanoscale Advances* 2023, **5**(21):5974-5982.

.53 Shqier R, Zyoud A, Helal MHS, Nassar H, Alkowni R, Assali M, Zyoud S, Qamhieh N, Hajamohideen AR, Sawalha S *et al*: **TiO2 nanopowder and nanofilm catalysts in the disinfection and mineralization of S. aureus with solar-simulated radiation**. *Reaction Chemistry & Engineering* 2024, **9**(7):1762-1775.

.54 Salameh N, Shraim N, Jaradat N, El Masri M, Adwan L, K'Aibni S, Alkowni R, Radwan A, AbuAlhasan M: **Screening of Antioxidant and Antimicrobial Activity of Micromeria fruticosa serpyllifolia Volatile Oils: A Comparative Study of**

Plants Collected from Different Regions of West Bank, Palestine. *Biomed Res Int* 2020, **2020**:4851879.

.55 Eid AM, Hawash M: **Biological evaluation of Safrole oil and Safrole oil Nanoemulgel as antioxidant, antidiabetic, antibacterial, antifungal and anticancer**. *BMC Complement Med Ther* 2021, **21**(1):159.

.56 Balouiri M, Sadiki M, Ibnsouda SK: **Methods for in vitro evaluating antimicrobial activity: A review**. *Journal of Pharmaceutical Analysis* 2016, **6**(2):71-79.

.57 Nassar MSM, Hazzah WA, Bakr WMK: **Evaluation of antibiotic susceptibility test results: how guilty a laboratory could be?** *The Journal of the Egyptian Public Health Association* 2019, **94**(1):4.

.58 Abualhasan M, Hawash M, Aqel S, Al-Masri M, Mousa A, Issa L: **Biological Evaluation of Xanthene and Thioxanthene Derivatives as Antioxidant, Anticancer, and COX Inhibitors**. *ACS Omega* 2023, **8**(41):38597-38606.

.59 Alharbi NS, Alsubhi NS: **Green synthesis and anticancer activity of silver nanoparticles prepared using fruit extract of Azadirachta indica**. *Journal of Radiation Research and Applied Sciences* 2022, **15**(3):335-345.

.60 Nie P, Zhao Y, Xu H: **Synthesis, applications, toxicity and toxicity mechanisms of silver nanoparticles: A review**. *Ecotoxicology and Environmental Safety* 2023, **253**:114636.

.61 Kaur B, Singh P: **Inflammation: Biochemistry, cellular targets, anti-inflammatory agents and challenges with special emphasis on cyclooxygenase-2**. *Bioorganic Chemistry* 2022, **121**:105663.

.62 Achour S, Khelifi E, Attia Y, Ferjani E, Helal AN: **Concentration of Antioxidant Polyphenols from Thymus capitatus extracts by Membrane Process Technology**. *Journal of Food Science* 2012, **77**.

.63 Mechchate H: **Chemical Composition, Antioxidant and Antibacterial Activities of Thymus broussonetii Boiss and Thymus capitatus (L.) Hoffmann and Link Essential Oils**. *Plants (Basel, Switzerland)* 2022, **11**(7):954.

.64 Zairi A, Nouir S, Zarrouk A, Haddad H, Khélifa A, Achour L, Tangy F, Chaouachi M, Trabelsi M: **Chemical composition, Fatty acids profile and Biological**

properties of Thymus capitatus (L.) Hoffmanns, essential Oil. *Scientific Reports* 2019, **9**:20134.

.65 Noureddine T, Benchikha N, Messaoudi M, Caruso G, Emran T, Atoki A, Adeniyi I: **Chemical composition and biological properties of Thymus capitatus plants from Algerian high plains: A comparative and analytical study**. *Open Chemistry* 2024, **22**.

.66 Benomari FZ, Sarazin M, Chaib D, Pichette A, Boumghar H, Boumghar Y: **Chemical Variability and Chemotype Concept of Essential Oils from Algerian Wild Plants**. 2023, **28**.(11)

.67 Goudjil M, Souad Z, Saoud D, Mahcene Z, Bencheikh se, Segni L: **Biological activities of essential oils extracted from Thymus capitatus (Lamiaceae)**. *South African Journal of Botany* 2019, **128**:274-282.

.68 Mikhailova EO: **Silver Nanoparticles: Mechanism of Action and Probable Bio-Application**. *J Funct Biomater* 2020, **11**.(4)

.69 Vinicius de Oliveira Brisola Maciel M, da Rosa Almeida A, Machado MH, Elias WC, Gonçalves da Rosa C, Teixeira GL, Noronha CM, Bertoldi FC, Nunes MR, Dutra de Armas R *et al*: **Green synthesis, characteristics and antimicrobial activity of silver nanoparticles mediated by essential oils as reducing agents**. *Biocatalysis and Agricultural Biotechnology* 2020, **28**:101746.

.70 Jiang XC, Chen WM, Chen CY, Xiong SX, Yu AB: **Role of Temperature in the Growth of Silver Nanoparticles Through a Synergetic Reduction Approach**. *Nanoscale research letters* 2011, **6**(1):32.

.71 Velgosová O, Mražíková A, Marcinčáková R: **Influence of pH on green synthesis of Ag nanoparticles**. *Materials Letters* 2016, **180**:336-339.

.72 Judith Vijaya J, Jayaprakash N, Kombaiah K, Kaviyarasu K, John Kennedy L, Jothi Ramalingam R, Al-Lohedan HA, V.M M-A, Maaza M: **Bioreduction potentials of dried root of Zingiber officinale for a simple green synthesis of silver nanoparticles: Antibacterial studies**. *Journal of Photochemistry and Photobiology B: Biology* 2017, **177**:62-68.

.73 Singh T, Jyoti K, Patnaik A, Singh A, Chauhan R, Chandel SS: **Biosynthesis, characterization and antibacterial activity of silver nanoparticles using an endophytic fungal supernatant of Raphanus sativus**. *Journal of Genetic Engineering and Biotechnology* 2017, **15**(1):31-39.

.74 Fissan H, Ristig S, Kaminski H, Asbach C, Epple M: **Comparison of different characterization methods for nanoparticle dispersions before and after aerosolization**. *Analytical Methods* 2014, **6**(18):7324-7334.

.75 Eaton P, Quaresma P, Soares C, Neves C, de Almeida MP, Pereira E, West P: **A direct comparison of experimental methods to measure dimensions of synthetic nanoparticles**. *Ultramicroscopy* 2017, **182**:179-190.

.76 Tiwari AK, Kumar A, Said Z: **Chapter 3 - Synthesis, characterization, and measurement techniques for the thermophysical properties of nanofluids**. In: *Advances in Nanofluid Heat Transfer.* Edited by Ali HM: Elsevier; 2022: 59-93.

.77 Sameeh MY: **An Overview of Nanoparticles from Medicinal Plants: Synthesis, Characterization and Bio-Applications**. *Advances in Bioscience and Biotechnology* 2023.(10)14

.78 Alsharif SM, Salem SS, Abdel-Rahman MA, Fouda A, Eid AM, El-Din Hassan S, Awad MA, Mohamed AA: **Multifunctional properties of spherical silver nanoparticles fabricated by different microbial taxa**. *Heliyon* 2020, **6**(5):e03943.

.79 Parvathaneni V, Goyal M, Kulkarni NS, Shukla SK, Gupta V: **Nanotechnology Based Repositioning of an Anti-Viral Drug for Non-Small Cell Lung Cancer (NSCLC)**. 2020, **37**(7):123.

.80 Melkamu WW, Bitew LT: **Green synthesis of silver nanoparticles using Hagenia abyssinica (Bruce) J.F. Gmel plant leaf extract and their antibacterial and anti-oxidant activities**. *Heliyon* 2021, **7**(11):e08459.

.81 Bajes H, Oran S, Bustanji Y: **Phytochemical Analysis, In vitro Assessment of Antioxidant Properties and Cytotoxic Potential of Thymus capitatus Essential Oil**. *Research Journal of Pharmacy and Technology* 2023:1100-1108.

.82 Wang S, Cheng Y, Wang J, Ding M, Fan Z: **Antioxidant Activity, Formulation, Optimization and Characterization of an Oil-in-Water Nanoemulsion Loaded**

with Lingonberry (Vaccinium vitis-idaea L.) Leaves Polyphenol Extract. *Foods* 2023.4256:(23)12 ,

.83 Moosavy M-H, de la Guardia M, Mokhtarzadeh A, Khatibi SA, Hosseinzadeh N, Hajipour N: **Green synthesis, characterization, and biological evaluation of gold and silver nanoparticles using Mentha spicata essential oil**. *Scientific Reports* 202.7230:(1)13 ,3

.84 Vega-Baudrit J, Gamboa SM, Rojas ER, Martinez VV: **Synthesis and characterization of silver nanoparticles and their application as an antibacterial agent**. *International Journal of Biosensors & Bioelectronics* 2019, **5**.(5)

.85 Vanlalveni C ,Lallianrawna S, Biswas A, Selvaraj M, Changmai B, Rokhum SL: **Green synthesis of silver nanoparticles using plant extracts and their antimicrobial activities: a review of recent literature**. *RSC Advances* 2021, **11**(5):2804-2837.

.86 Küp FÖ, Çoşkunçay S, Duman F: **Biosynthesis of silver nanoparticles using leaf extract of Aesculus hippocastanum (horse chestnut): Evaluation of their antibacterial, antioxidant and drug release system activities**. *Materials Science and Engineering: C* 2020, **107**:110207.

.87 Singh J ,Kumar A, Nayal AS, Vikal S, Shukla G, Singh A, Singh A, Goswami S, Kumar A, Gautam YK *et al*: **Comprehensive antifungal investigation of green synthesized silver nanoformulation against four agriculturally significant fungi and its cytotoxic applications** .*Scientific Reports* 2024, **14**(1):5934.

.88 Du H, Lo T-M, Sitompul J, Chang MW: **Systems-level analysis of Escherichia coli response to silver nanoparticles: The roles of anaerobic respiration in microbial resistance**. *Biochemical and Biophysical Research Communications* 2012, **424**(4):657-662.

.89 Abass Sofi M, Sunitha S, Ashaq Sofi M, Khadheer Pasha SK, Choi D: **An overview of antimicrobial and anticancer potential of silver nanoparticles**. *Journal of King Saud University - Science* 2022, **34**(2):101791.

.90 Kovács D, Igaz N: **Cancer Therapy by Silver Nanoparticles: Fiction or Reality?** 2022, **23**.(2)

.91 Sur I, Çam D, Kahraman M, Baysal A, Culha M: **Interaction of Multi-Functional Silver Nanoparticles with Living Cells**. *Nanotechnology* 2010, **21**:175104.

.92 Eid AM, Jaradat N, Shraim N, Hawash M, Issa L, Shakhsher M, Nawahda N, Hanbali A, Barahmeh N, Taha B *et al*: **Assessment of anticancer, antimicrobial, antidiabetic, anti-obesity and antioxidant activity of Ocimum Basilicum seeds essential oil from Palestine**. *BMC Complement Med Ther* 2023, **23**(1):221.

.93 Kuffel MJ, Ames MM: **Comparative resistance of idarubicin, doxorubicin and their C-13 alcohol metabolites in human MDR1 transfected NIH-3T3 cells**. *Cancer Chemotherapy and Pharmacology* 1995, **36**(3):223-226.

.94 Bulut I, Lee A ,Cevatemre B, Ruzic D, Belle R, Kawamura A, Gul S, Nikolic K, Ganesan A, Acilan C: **Dual LSD1 and HDAC6 Inhibition Induces Doxorubicin Sensitivity in Acute Myeloid Leukemia Cells**. *Cancers* 2022, **14**(23):6014.

.95 Merino M, Lozano T, Casares N, Lana H, Troconiz IF, ten Hagen TLM, Kochan G, Berraondo P, Zalba S, Garrido MJ: **Dual activity of PD-L1 targeted Doxorubicin immunoliposomes promoted an enhanced efficacy of the antitumor immune response in melanoma murine model**. *Journal of Nanobiotechnology* 2021, **19**(1.102:(

.96 Gomathi AC, Xavier Rajarathinam SR, Mohammed Sadiq A, Rajeshkumar S: **Anticancer activity of silver nanoparticles synthesized using aqueous fruit shell extract of Tamarindus indica on MCF-7 human breast cancer cell line**. *Journal of Drug Delivery Science and Technology* 2020, **55**:101376.

.97 Gopisetty MK, Kovács D, Igaz N, Rónavári A, Bélteky P, Rázga Z, Venglovecz V, Csoboz B, Boros IM, Kónya Z *et al*: **Endoplasmic reticulum stress: major player in size-dependent inhibition of P-glycoprotein by silver nanoparticles in multidrug-resistant breast cancer cells**. *Journal of Nanobiotechnology* 2019, **17**(1):9.

.98 Bakrania A, Zheng G, Bhat M: **Nanomedicine in Hepatocellular Carcinoma: A New Frontier in Targeted Cancer Treatment**. *Pharmaceutics* 2022, **14**(1):41.

.99 Soares CLR, Wilairatana P, Silva LR, Moreira PS, Vilar Barbosa NMM, da Silva PR, Coutinho HDM, de Menezes IRA, Felipe CFB: **Biochemical aspects of the**

inflammatory process: A narrative review. *Biomedicine & Pharmacotherapy* 2023, **168**:115764.

.100 Chen L ,Deng H, Cui H, Fang J, Zuo Z, Deng J, Li Y, Wang X, Zhao L: **Inflammatory responses and inflammation-associated diseases in organs**. *Oncotarget* 2018, **9**(6):7204-7218.

.101 Yang B, Dong Y, Wang F, Zhang Y: **Nanoformulations to Enhance the Bioavailability and Physiological Functions of Polyphenols**. *Molecules* 2020, **25**(20):4613.

.102 Seethalakshmi S AMKM: **Evaluation of In-vitro Anti-Inflammatory Activity of Silver Nanoparticles Synthesised using Piper Nigrum Extract**. *Journal of Nanomedicine & Nanotechnology* 201.(02)06 ,5

.103 Khashan AA, Dawood Y, Khalaf YH: **Green chemistry and anti-inflammatory activity of silver nanoparticles using an aqueous curcumin extract**. *Results in Chemistry* 2023, **5**:100913.

Appendices

Appendix A

GC_MS Analysis Results

Figure A.1

GC-MS analysis results of T.capitatus EO

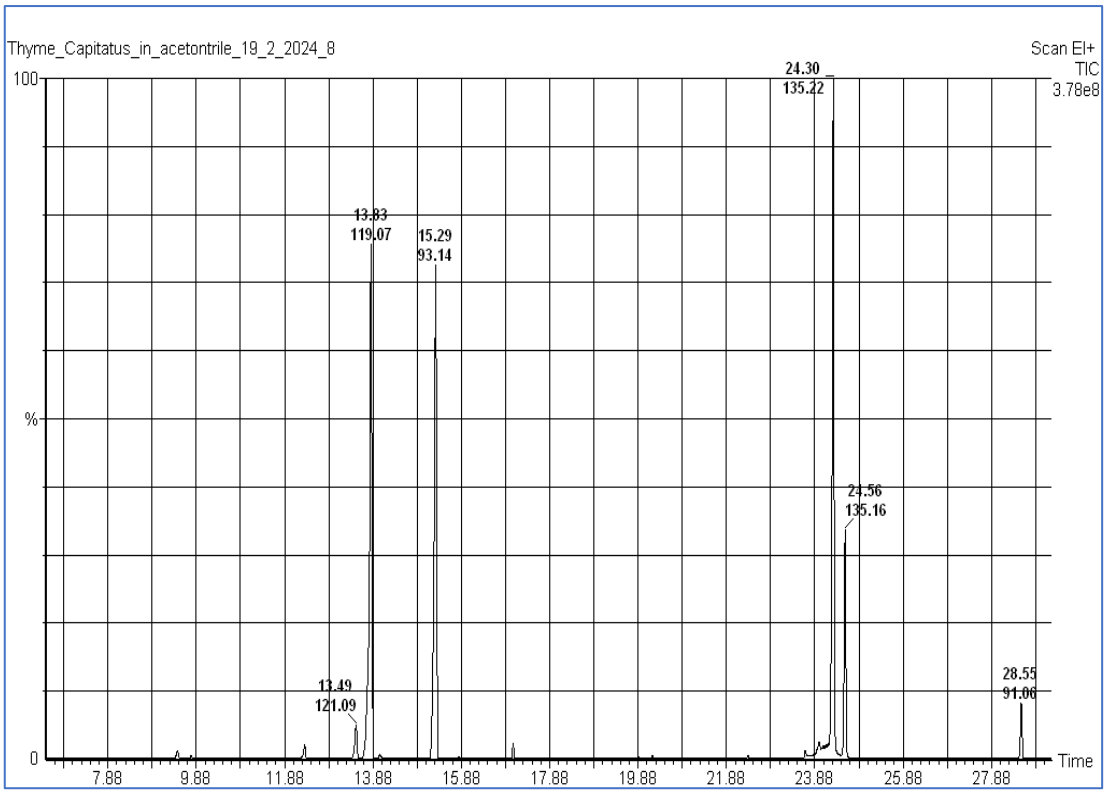

Figure A2

Chemical composition of the Palestinian T. capitatus EO according to a thesis study that was previously done

Table 3.2.1

GC-MS analysis results

Ramalla	Rt	RI	%	Jenin	Rt	RI	%	Hebron	Rt	RI	%
α-Thujene	8.403	925	0.65	α-Thujene	8.415	926	0.31	********	***	***	***
a-Pinene	8.71	933	0.7	a-Pinene	8.695	933	0.49	a-Pinene	8.7	933	2.52
Camphene	9.37	949	0.15	Camphene	9.35	949	0.9	Camphene	9.351	949	5.56
Sabinene	10.501	976	0.17	b-pinene	10.486	976	0.49	b-pinene	10.501	976	0.23
Myrcene	11.07	990	0.73	Myrcene	11.06	990	0.33	Myrcene	11.071	990	0.17
a-Phellandrene	11.71	1006	0.08	α-Terpinene	12.157	1017	1.41	α-Terpinene	12.162	1017	0.35
α-Terpinene	12.167	1017	2.25	p-Cymene	12.49	1025	1.41	p-Cymene	12.487	1025	8.41
o-Cymene	12.507	1025	16.84	γ-Terpinene	13.887	1059	67	Limonene	12.672	1029	0.47
Sylvestrene	12.687	1029	0.4	cis-4-thujanol	15.608	1101	0.19	γ-Terpinene	13.887	1060	3.61
γ-Terpinene	13.91	1059	30.94	cis-b-Terpineol	18.698	1181	12.91	cis-4-thujanol	15.603	1101	2.98
linalool	15.903	1109	6.19	carvacrol methyl ether	20.86	1240	0.07	Camphor	17.389	1147	0.004
cis-b-Terpineol	18.674	1181	0.02	2-Isopropyl-4-methylphenol	21.78	1266		2-Methyl isoborneol	18.389	1173	2.24
thymol methy ether	20.825	1239	0.24	o-cymenol	21.996	1278	0.14	Terpinene-4-ol	18.689	1181	0.02
thymol	22.131	1276	3	thymol	22.776	1293	5.51	a-Terpineol	19.286	1196	0.23
carvacrol	23.136	1304	31.25	carvacrol	23.056	1301	6.44	**********	20.465	1229	0.58
b-Caryophellene	26.988	1420	4.61	b-Caryophellene	26.993	1419	1.65	Carvacrol, methyl eth	20.855	1240	10.7
	27.608	1440	0.28	trans-a-Bergamotene	27.618	1440	0.1	Isobornyl acetate	22.461	1285	0.38
α-Caryophyllene	28.143	1457	0.19	α-Caryophyllene	28.14	1457		thymol	22.771	1293	40.35
Viridiflorene	29.284	1493	0.27	Caryophellene oxide	32.03	1585	0.11	carvacrol	23.056	1301	0.58
Caryophellene oxide	32.035	1586	o.77					b-Caryophellene	26.993	1420	13.23
								Caryophellene oxide	32.02	1585	1.8
Sum			98.96				99.35				92.61

Table A.1

Chemical composition of the Algerian T. capitatus EO

Compounds	RT	*T. Capitatus%*
α-thujene	1,716	0,38
α-Pinene	1,804	0,91
Camphene	1,99	0,2
β-Myrcene	2,465	1,49
α-terpinene	2,852	1,78
γ -Terpinene	3,479	10,3
Linalool	4,047	2,29
Terpineol	6,52	0,37
Thymol	7,557	51,22
Carvacrol	8,038	12,59
α-gurjunene	8,335	0,26
Caryophyllene	8,53	2,01
(+)-Ledene	9,372	0,34
β-Bisabolene	9,589	0,3
β-copaene	9,64	0,12
delta-Amorphene	9,703	0,24
α-Bisabolene	9961	0,23
Elemicin	10,057	0,14
(-)-Spathulenol	10,434	0,87
Caryophyllene oxide	10,461	1,21
Pentadecanoic acid	14,564	1,92
trans-13-Octadecenoic acid	16,414	9,04
Total		98,21

RI : retention indices relative

جـامعـــة النجاح الوطنية

كليـــة الدراســـات العليـــا

تصنيع وتوصيف جزيئات الفضة النانوية باستخدام نبات الزعتر الفارسي الفلسطيني، مع تقييم فعاليته كمضادات للأكسدة ومضادات للميكروبات ومضادات السرطان ومضادات الالتهاب

إعداد

لارا ياسر فوزي اسمر

إشراف

د احمد عيد

قدمت هذه الرسالة استكمالا لمتطلبات الحصول على درجة الماجستير في العلوم الصيدلانية، من كلية الدراسات العليا، في جامعة النجاح الوطنية، نابلس– فلسطين.

2025

تصنيع وتوصيف جزيئات الفضة النانوية باستخدام نبات الزعتر الفارسي الفلسطيني، مع تقييم فعاليته كمضادات للأكسدة ومضادات للميكروبات ومضادات السرطان ومضادات الالتهاب

إعداد

لارا ياسر فوزي أسمر

إشراف

د. احمد عيد

الملخص

قدمت هذه الأطروحة إمكانية تخليق جسيمات الفضة النانوية باستخدام الزيت العطري لنبات الزعتر الفارسي الفلسطيني ودراسة النشاطات الحيوية المحتملة لهذه الجسيمات، تم استخلاص الزيت بتقنية التقطير المائي، وتم استخدام جهاز مقياس الطيف الكتلي لتحديد التركيب الكيميائي له، وكانت المركبات الرئيسية كالتالي: الكارفاكرول بنسبه(37.47%) ، البارا–سيمين بنسبه (27.96%) ، والجاما–تيربينين بنسبه (26.3%).

تحقق التخليق الأمثل الجسيمات الفضة النانوية من خلال إضافة الزيت المخفف بمادة الاستون إلى محلول نترات الفضة المائي بتركيز 0.1 مولار بالتنقيط تحت تحريك مغناطيسي متوسط بدرجة حرارة الغرفة. وكان تغير لون المحلول إلى البني الداكن هو المؤشر الاول لتكوّن الجسيمات النانوية، وأكد مطياف الأشعة فوق االبنفسجية–المرئية على تكونها ايضا حيث تم الحصول على ذروة الطيف عند 425 نانومتر. أظهر جهاز مجهر القوة الذرية AFM جسيمات الفضه النانونيه بشكل كروي، تراوح حجمها مابين 40 و80 نانومترا.

تم تطبيق العديد من الاختبارات المختبرية لتحديد النشاط البيولوجي المحتمل لكل من الجسيمات الفضة النانوية و الزيت النقي، اثبت اختبار مضادات الأكسدة ان كلاهما يمتلكان مضادات أكسدة جيدة مقارنةً بمادة ترولكس، حيث بلغت قيم ال C50 48.97±1.20 امايكرو غرام/مل للزيت و10.47+– 1.11 مايكرو غرام للجسيمات النانونيه، و2.27 +– 0.91 مايكروغرام/مل لماده الترولوكس. كما وأظهرت النتائج

أن الجسيمات النانويه تمتلك نشاطا مضادا للمايكروبات يفوق نشاط الزيت المستخلص بخمسة أضعاف، وذلك ضد جميع السلالات البكتيرية المستخدمة في الدراسة، حيث تراوحت قيم التركيز المثبط الادنى مابين (0.016 و 0.29 ميكروغرام/مل) للجسيمات النانوية، و(0.078 و 1.562 ميكرو غرام/مل) للزيت.

كما أظهرت النتائج ان كلا من الجسيمات النانوية والزيت يمتلكان فعالية ممتازة ضد الخلايا السرطانية المستخدمة في الدراسة،و بلغت قيم التثبيط النصفي لهذه الجسيمات ضد خلايا الكبد السرطانيه22.38 ميكروغرام/مل ، وضد خلايا سرطان الثدي 22.9 ميكروغرام/مل ، وضد الخلايا الليفيه الجنينيه للفار 18.19 ميكروغرام/مل، وضد خلايا سرطان عنق الرحم 25.11 ميكروغرام/مل، وضد خلايا الكلية الجنينية البشرية 18.19 ميكروغرام/مل ، وضد خلايا سرطان الجلد في الفئران 27.54 ميكروغرام/مل. أظهرت النتائج ان جسيمات الفضه النانوية ذات تاثير قوي على انزيمات الاكسده الحلقيه −2 مقارنه بتاثيرها على انزيمات الاكسده الحلقيه −1 بمقدار تثبيط نصفي 2.83 ميكروغرام/مل ، حيث ان هذه القيمة تمثل 14% من قيمة التثبيط النصفي لدواء الكيتوبروفين والتي بلغت 40.18 ميكروغرام/مل .

تشير نتائج هذه الدراسه بشكل عام إلى إمكانية استخدام هذه الجسيمات النانوية في مجالات طبيه مختلفة خاصة لعلاج بعض امراض السرطان، بهدف تحسين الفعالية و تقليل الآثار الجانبية للادوية.

الكلمات المفتاحية: الزعتر الفارسي، مضادات الاكسدة، جزيئات الفضة النانوية، مضادات البكتيريا، مضادات السرطان.